JCI The Journal of Clinical Investigation

Epithelial splicing regulatory protein 2-mediated alternative splicing reprograms hepatocytes in severe alcoholic hepatitis

Jeongeun Hyun, … , Auinash Kalsotra, Anna Mae Diehl

J Clin Invest. 2020. https://doi.org/10.1172/JCI132691.

Research In-Press Preview Cell biology Hepatology

Graphical abstract

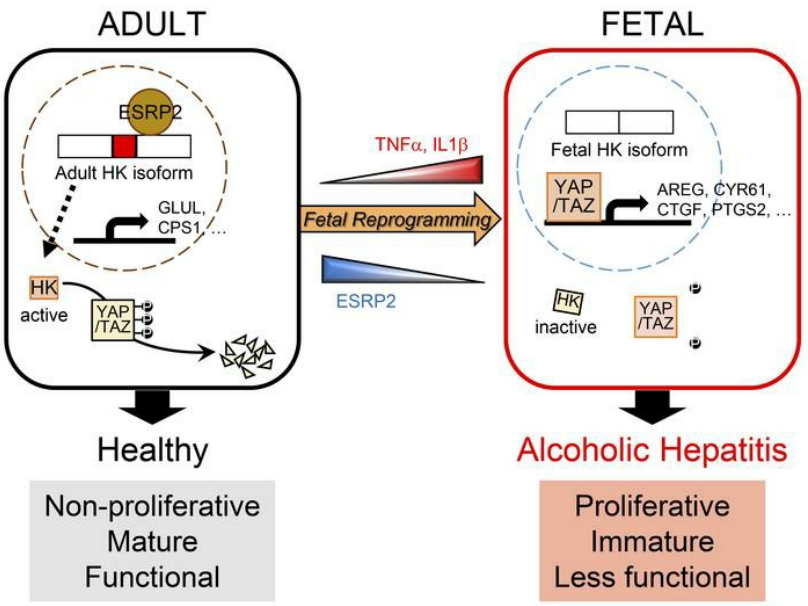

Epithelial splicing regulatory protein 2-mediated alternative splicing reprograms hepatocytes in severe alcoholic hepatitis

Jeongeun Hyun[1,2], Zhaoli Sun[3], Ali Reza Ahmadi[3], Sushant Bangru[4,5], Ullas V. Chembazhi[4], Kuo Du[1], Tianyi Chen[7], Hidekazu Tsukamoto[8,9], Ivan Rusyn[10], Auinash Kalsotra[4,5,6*], Anna Mae Diehl[1*]

[1]Department of Medicine, Duke University, Duke University Health System, Durham, NC, USA; [2]Regeneration Next, Duke University School of Medicine, Durham, NC, USA; [3]Department of Surgery, Johns Hopkins University School of Medicine, Baltimore, MD, USA; [4]Department of Biochemistry, University of Illinois Urbana-Champaign, Urbana, IL, USA; [5]Cancer Center@ Illinois, University of Illinois Urbana-Champaign, Urbana, IL, USA; [6]Carl R. Woese Institute of Genomic Biology, University of Illinois Urbana-Champaign, Urbana, IL, USA; [7]Department of Molecular Genetics and Microbiology, Duke University, Durham, NC, USA; [8]Southern California Research Center for ALPD and Cirrhosis and Department of Pathology, Keck School of Medicine of the University of Southern California; [9]Department of Veterans Affairs Greater Los Angeles Healthcare System, Los Angeles, CA, USA; [10]Department of Veterinary Integrative Biosciences, Texas A&M University, College Station, TX, USA

*Co-corresponding authors

Lead Contact: Anna Mae Diehl, M.D.

905 S LaSalle St., GSRB I, suite 1073, Durham, NC 27710

Phone: 1-919-684-4173; FAX: 1-919-684-4183; E-mail: annamae.diehl@duke.edu

Conflict of interest statement

The authors have declared that no conflict of interest exists.

Abbreviations

AdGFP, adenovirus-expressing green fluorescent protein; CPS1, carbamoyl-phosphate synthase-1; CDH1, cadherin-1; C/EBPα, CCAAT enhancer binding protein alpha; DDC, 3.5-Diethoxycarbonyl-1.4-dihydrocollidine; EMT, epithelial-to-mesenchymal transition; ESRP2, epithelial splicing regulatory protein-2; EXP, expansion; GLS2, glutaminase-2; GLUL, glutamate-ammonia ligase; HF, high fat; HK, hippo kinase; IGF2BP3, insulin-like growth factor-2 mRNA-binding protein-3; IL1β, interleukin-1 beta; IHC, immunohistochemistry; IND, induction; INR, international normalized ratio; KEGG, Kyoto Encyclopedia of Genes and Genomes; KO, knockout; NIAAA, National Institute on Alcohol Abuse and Alcoholism; PH, partial hepatectomy; PSI, percent spliced in; PT, prothrombin time; qRT-PCR, quantitative reverse transcription polymerase chain reaction; RBP, RNA-binding protein; SAH, severe alcoholic hepatitis; TNFα, tumor necrosis factor alpha; SMAD3, SMAD family member 3; SOX9, SRY (sec determining region Y)-box transcription factor-9; TNFRSF12A, TNF receptor superfamily member 12a; TAZ, tafazzin; WT, wild type; YAP, yes-associated protein

Keywords: alcoholic hepatitis, liver failure, epithelial splicing regulatory protein-2 (ESRP2), tumor necrosis factor alpha (TNFα), Hippo signaling pathway, YAP/TAZ, epithelial-to-mesenchymal transition (EMT), alternative splicing, fetal reprogramming, hepatocyte dedifferentiation

Abstract

Severe alcoholic hepatitis (SAH) is a deadly liver disease without an effective medical therapy. Although SAH mortality is known to correlate with hepatic accumulation of immature liver cells, why this occurs, and how it causes death is unclear. Here, we demonstrated that expression of epithelial splicing regulatory protein-2 (ESRP2), an RNA splicing factor that maintains the non-proliferative, mature phenotype of adult hepatocytes, was suppressed in both human SAH and various mouse models of SAH in parallel with the severity of alcohol consumption and liver damage. Inflammatory cytokines released by excessive alcohol ingestion reprogrammed adult hepatocytes into proliferative, fetal-like cells by suppressing ESRP2. Sustained loss of ESRP2 permitted re-emergence of a fetal RNA splicing program that attenuates the Hippo signaling pathway and thus, allows fetal transcriptional regulators to accumulate in adult liver. We further showed that depleting ESRP2 in mice exacerbated alcohol-induced steatohepatitis, enabling surviving hepatocytes to shed adult hepatocyte functions and become more regenerative but threatens overall survival by populating the liver with functionally-immature hepatocytes. Our findings revealed a novel mechanism that explains why liver failure develops in patients with the clinical syndrome of SAH, suggesting that recovery from SAH might be improved by limiting adult-to-fetal reprogramming in hepatocytes.

Introduction

Severe alcoholic hepatitis (SAH) is an alcohol-related liver disease with a short-term mortality rate approaching 50% and propensity for rapid progression to cirrhosis in survivors (1-3). The major causes of early death in SAH are hepatic failure and infection (2-4). Previous studies have shown that short-term mortality in SAH correlates with the accumulation of proliferative liver cells that express stem/progenitor cell markers via a process called the “ductular reaction” (5-7). Hence, fatal liver failure in SAH may be caused by excessive repopulation of the liver by fetal-like proliferative liver cells that lack mature hepatocyte functions and thus, inhibiting their accumulation would be therapeutic. However, this is not yet feasible because what causes fetal-like cells to accumulate in the livers of SAH patients is unknown.

Single-cell gene expression analysis recently demonstrated that feeding alcohol to adult rats increased the proportion of hepatocytes that are either becoming proliferative or proliferating (8), suggesting that excessive alcohol drinking might promote some degree of hepatocyte dedifferentiation. Maintaining hepatocytes in a differentiated state is a critical function of the Hippo-YAP signaling pathway (9). Hippo signaling promotes phosphorylation and degradation of YAP and TAZ, transcriptional regulators which drive organ growth during fetal development and promote cell proliferation and epithelial-to-mesenchymal transitions (EMT) essential for adult tissue regeneration (10). In healthy adult livers, Hippo signaling activity is high, keeping YAP/TAZ inactive and permitting mature hepatocyte transcription factors, such as C/EBPα (11), to control gene expression. In contrast, Hippo signaling activity is low in fetal livers, and this enables YAP/TAZ activity. Experiments in mice have shown that deleting *Nf2*, a component of the Hippo signaling pathway, or directly activating YAP in adult hepatocytes causes them to de-differentiate into proliferative ductal-like cells (9). Reintroducing Hippo signaling reverses this process and permits the reprogrammed hepatocytes to differentiate back to their basal non-replicative phenotype (9).

It was shown that the activity of two key components of Hippo signaling pathway, *Nf2* and *Csnk1d*, is controlled by an adult RNA splicing factor, epithelial splicing regulatory protein-2 (ESRP2) (12). By retaining exons to generate longer adult mRNAs, ESRP2 converts the fetal splicing variants which encode low kinase activity NF2 and CSNK1D proteins into adult splicing variants that encode kinases with higher activity to suppress YAP/TAZ (12). ESRP2 is absent in fetal livers but begins to be expressed in hepatocytes shortly after birth (13). It is critically important for switching on the adult splicing program in ~ 20% of hepatocyte mRNAs, generating splicing variants that encode functional differences in multiple proteins (13). Importantly, ESRP2 targets critically control hepatocyte proliferative activity because adult ESRP2 knockout (KO) mice demonstrate significantly increased rates of hepatocyte proliferation (13). ESRP2 is also known to be downregulated during EMT (14, 15), permitting fetal splicing variants of EMT-related genes to accumulate.

The potential role of ESRP2 as a key regulator of hepatocyte maturation is supported by the finding that expression of ESRP2 is suppressed as non-replicating mature hepatocytes transition to become proliferative after 70% partial hepatectomy (PH) but promptly recovers back to baseline as regeneration is completed (16). Indeed, hepatocytes that are becoming proliferative accumulate excessively in livers of alcohol-fed rats after PH and alcohol prevented maturation of hepatocytes (8), explaining why liver regeneration is inhibited by alcohol (17, 18). However, the mechanisms involved were not defined. The present study evaluates the hypothesis that the ESRP2-mediated adult splicing program is inactivated in some individuals with alcohol-induced liver injury, causing extensive repopulation of SAH livers with immature, fetal-like cells. The results identify the mechanism for liver failure in SAH by revealing that TNFα and IL1β (19), pro-inflammatory cytokines that accumulate in alcohol-injured livers, suppress ESRP2 in adult hepatocytes. Loss of ESRP2 permits relatively inactive fetal splicing variants of Hippo kinases to accumulate and enables the reactivation of YAP/TAZ, which then reprogram hepatocytes to become more proliferative, but less capable of performing vital, mature hepatocyte functions.

Results

Adult-to-fetal reprogramming occurs in livers of patients with SAH

To examine whether adult-to-fetal reprogramming occurs in human livers during the pathogenesis of SAH, we leveraged knowledge about transcription factor switching during normal development. As the liver matures, progressive activation of adult hepatocyte transcription factors, such as C/EBPα, suppresses the expression of genes that promote hepatocyte proliferation, but induces the expression of genes that accomplish mature liver functions (11). Conversely, YAP and TAZ, transcriptional regulators that are active in fetal livers, become silenced by progressive increases in Hippo signaling activity as the liver matures. Thus, C/EBPα localizes within nuclei of healthy adult hepatocytes, but YAP and TAZ are barely detectable (Figure 1A). In contrast, almost none of the hepatocyte nuclei express C/EBPα, but both YAP and TAZ are abundant, in explanted livers of adult patients who underwent liver transplantation for SAH (Figure 1A), suggesting that hepatocytes de-differentiate during SAH. Since YAP and TAZ have been shown to induce stem cell characteristics and EMT (10), we also examined the expression of two liver progenitor markers, TNFRSF12A (also known as FN14) (20) and SOX9 (21), and two important EMT-related factors, SMAD3 and CDH1 (also known as E-Cadherin) (15). While TNFRSF12A, SOX9 and the EMT inducer, SMAD3, are rarely detected in healthy liver, livers of SAH patients are enriched with cells expressing these progenitor and mesenchymal markers. Conversely, CDH1, an adherens junction protein that maintains epithelial integrity in healthy liver (22), is lost from hepatocytes of SAH patients (Supplemental Figure 1).

To more globally assess SAH-associated changes in liver cell phenotypes, we performed KEGG pathway analysis using transcriptome profiles obtained by RNA sequencing (RNA-seq) of explanted livers of five SAH patients and five controls without known liver disease. Genes responsible for mature hepatocyte functions, including synthesis of clotting factors and multiple metabolic pathways, are suppressed in SAH livers (Figure 1B and Supplemental Figure 2). In contrast, the Notch pathway which drives cells in developing livers to become ductal-like (23) is

up-regulated, as are genes involved in cancer and chemokine signaling pathways (Figure 1B and Supplemental Figure 2). These findings support the concept that adult-to-fetal reprogramming occurs in human SAH livers.

ESRP2-controlled adult RNA splicing program is suppressed in human SAH

Recently, we discovered that ESRP2 controls the adult splicing program of mRNAs that encode two key components of the Hippo kinase (HK) cascade, CSNK1D and NF2, preserving their activities to phosphorylate and degrade YAP and TAZ in mature hepatocytes (12). Therefore, we examined these ESRP2-mediated splicing events to address how YAP and TAZ are re-activated in liver tissues of adult SAH patients. We found that expression of ESRP2 is significantly downregulated at both the levels of mRNA and protein in livers of SAH patients compared to a healthy liver (Figure 2A-D). In addition, ESRP2 is mis-localized, being restricted to cell cytosol in SAH livers while localizing in hepatocyte nuclei of the healthy liver (Figure 2D). The loss of ESRP2 in SAH livers associated with accumulation of smaller (fetal) splicing variants of the HK mRNAs, CSNK1D and NF2, at the expense of longer (adult) splicing variants of these transcripts (Figure 2E), as evidenced by a fall in the percentage of total transcripts with exons spliced in (Percent Spliced In, PSI) (Figure 2E). Consistent with reduced kinase activity of HKs encoded by fetal CSNK1D and NF2, YAP and TAZ activity is increased in SAH livers, as demonstrated by upregulation of YAP/TAZ direct target genes (AREG (24), CYR61 (25), CTGF (26, 27), PTGS2 (28)) (Figure 2A,B). Fetal splicing variants of SLK and FLNB, two additional ESRP2 targets which encode proteins involved in EMT (29-31), also accumulate in SAH livers (Figure 2E). These results demonstrate that ESRP2 simultaneously regulates multiple targets to enrich adult hepatocytes with proteins that they require to accomplish vital liver-specific functions, while limiting the production of proteins involved in proliferation, migration and morphogenesis, functions that are unnecessary in healthy adult livers.

Interestingly, in human SAH down-regulation of ESRP2 (an adult RNA binding protein (RBP)) associated with up-regulation of a YAP-dependent fetal RBP that promotes stem/progenitor-like traits in liver cells, insulin-like growth factor-2 mRNA-binding protein-3 (IGF2BP3) (16) (Figure 2F-H). Whether cells exhibit fetal or adult phenotypes is controlled by families of coordinately-regulated RNA binding proteins (RBPs) that regulate the stability, translation, and splicing of mRNAs. Altogether, these data indicate that adult hepatocytes are reprogrammed to become more fetal-like during SAH and suggest that this dedifferentiation process is mediated, at least in part, by re-activation of a fetal RNA splicing program that emerges when the adult splicing factor, ESRP2, is suppressed.

Adult-to-fetal reprogramming responses correlate with the severity of inflammatory liver damage in mouse models of alcoholic liver disease

Since preclinical models are necessary to determine if and how misregulated hepatocyte reprogramming causes liver failure, we screened liver samples from different mouse models of alcoholic hepatitis (AH) to assess whether these models recapitulate the adult-to-fetal reprogramming that occurs in human SAH livers. We demonstrated fetal reprogramming responses reminiscent of those observed in human SAH in the Tsukamoto-French mouse model which uses a protracted high-fat diet/intragastric ethanol infusion protocol to generate severe inflammatory liver injury and moderate liver fibrosis (32) (Supplemental Figure 3). This AH model suppresses *Esrp2* expression, promotes relative accumulation of fetal- (versus adult) splicing variants of mRNAs encoding both HKs and genes controlling cell proliferation and differentiation (*Slk* and *Kras* (13)), and increases YAP/TAZ activity as evidenced by induction of their target genes including *Areg*, *Birc5* (33) and *Itgb2* (26) (Supplemental Figure 3).

We found that some of the human SAH-like reprogramming responses also occur in three other models of alcohol-induced liver injury, (i) the Gao binge model of chronic (10 days) plus acute alcohol binging (also known as the NIAAA model), (ii) the Lieber DeCarli high fat diet model of

voluntary chronic alcohol diet consumption followed by binging, and (iii) the long-term high fat (HF)/DDC diet plus alcohol feeding model. In these models, alcohol feeding promotes suppression of *Esrp2* and adult splicing variants relative to pair-fed or HF/DDC diet-fed control mice (Supplemental Figure 4). However, liver injury is much milder in these models than in the Tsukamoto-French SAH model or human SAH. Effects on *Esrp2*, splicing variants (Supplemental Figure 4), and YAP/TAZ target genes are also less profound (data not shown). Therefore, the aggregate data suggest that the level of ESRP2 suppression and adult-to-fetal reprogramming parallel the severity of liver injury (and thus the level of regenerative challenge). Further, the PSI indexes inversely correlate with the levels of blood alcohol and the histologic severity of liver inflammation in the Tsukamoto-French AH model (Figure 3), suggesting that accumulation of fetal splicing variants might be influenced by tractable factors that drive SAH pathogenesis.

Pro-inflammatory cytokines reprogram hepatocytes into fetal-like cells by suppressing the ESRP2-mediated adult splicing program

Excessive exposure to macrophage-derived pro-inflammatory cytokines, such as TNFα and IL1β, is critically involved in SAH pathogenesis (34) and SAH mortality is known to correlate with accumulation of fetal-like liver cells (5, 6). Therefore, we designed experiments to test if macrophage-derived factors regulate *Esrp2* expression in hepatocytes. We co-cultured AML12 adult mouse hepatocytes with RAW264.7 mouse macrophages in trans-wells and discovered that this both increases hepatocyte exposure to TNFα, and suppresses hepatocyte expression of *Esrp2* (Supplemental Figure 5A,B). In subsequent studies, we treated AML12 monocultures with TNFα, IL1β, or TNFα + IL1β and found that these inflammatory cytokines directly suppress *Esrp2* expression (Supplemental Figure 5C). Loss of ESRP2 activity is also evident since both cytokines stimulate the accumulation of fetal splicing variants of HK mRNA (*Csnk1d*) or EMT-related genes (*Slk*, *Flnb*) (Supplemental Figure 5D), and promote activation of YAP/TAZ as evidenced by

induction of their target gene (*Ptgs2*) (Supplemental Figure 5E). Importantly, cytokine-induced reprogramming responses associate with increased hepatocyte growth (Supplemental Figure 5F).

TNFα was recently reported to induce fetal liver cell traits in primary hepatocytes from healthy adult mice, including the ability to propagate *ex vivo* indefinitely as spheroids (35). Further, when transplanted into recipient mice with injured livers, these fetal-like hepatocytes were shown to repopulate the livers and eventually differentiate into mature, fully functional hepatocytes, proving that "switching" adult-to-fetal/fetal-to-adult programs on and off in hepatocytes is critically important for adult liver regeneration. However, neither the mechanisms driving TNFα-dependent dedifferentiation, nor those that permitted hepatocytes to re-differentiate when TNFα dissipates, were described. We used this TNFα-dependent spheroid system to evaluate if and how growth under these conditions influenced ESRP2-regulated mechanisms controlling adult-to-fetal hepatocyte reprogramming (Supplemental Figure 6A). Compared to freshly isolated mouse primary hepatocytes, primary adult hepatocytes that were exposed to inflammatory cytokines and grown as spheroids exhibited profound suppression of *Esrp2*, accumulation of fetal RNA splicing variants (i.e., decreased PSI) and induction of YAP/TAZ target genes (Figure 4A-C). Consistent with this finding, immuno-fluorescent staining showed that both YAP and TAZ translocated into hepatocyte nuclei upon TNFα and IL1β stimulation (Figure 4D and Supplemental Figure 6B). To assess the reproducibility of these novel results, we analyzed available online single cell RNA-seq (scRNA-seq) data that others derived from similar hepatocyte spheroids (35). Freshly isolated primary hepatocytes ("PRIMARY") strongly express *Esrp2,* but transcripts of YAP/TAZ target genes (e.g., *Areg* or *Ptgs2)* are not detectable (Figure 4E). In comparison, hepatocytes that are *expanding* to form spheroids in TNFα-enriched conditions ("EXP") decrease *Esrp2* expression but increase the expression of *Areg* and *Ptgs2* (Figure 4E). Remarkably, hepatocyte spheroids recover levels of *Esrp2* expression that approach those of freshly isolated primary hepatocytes after being cultured for 4 days in TNFα-depleted hepatocyte differentiation-*inducing* medium

("IND") (Figure 4E). Moreover, none of the hepatocytes that re-acquire adult levels of *Esrp2* (relative expression level > 1.0) co-express YAP/TAZ target genes (e.g., *Areg* and *Ptgs2)* (Supplemental Figure 6C).

To investigate whether restoration of ESRP2 in hepatocyte spheroids under "IND" culture conditions suppresses YAP/TAZ activity by retrieving the adult RNA splicing program, we transduced adenoviruses expressing mouse *Esrp2* (AdESRP2) into primary hepatocyte spheroids that we generated using the TNFα-dependent conditions. We found that increasing *Esrp2* levels promotes accumulation of adult (high PSI) splicing variants of HK mRNAs and EMT-related genes (including *Flnb* and *Kras*) (Figure 5A-C) and decreases YAP/TAZ activity, as evidenced by reduced expression of their target genes (Figure 5A), indicating that TNFα and IL1β stimulate hepatocytes to become fetal-like by switching off the ESRP2-mediated adult RNA splicing program.

Excessive accumulation of fetal-like hepatocytes causes liver failure

To assess potential functional consequences of excessive adult-to-fetal reprogramming in injured adult livers, we compared ammonia detoxification in freshly isolated adult hepatocytes and fetal-like hepatocyte spheroids because hyperammonemia is common, and predicts acute mortality (36), in humans with SAH, and ammonia accumulation promotes hepatic encephalopathy, a defining feature of liver failure in humans (36, 37). Healthy adult hepatocytes detoxify ammonia by converting it into either urea (via carbamoyl-phosphate synthase-1, CPS1) or glutamine (via glutamate-ammonia ligase, GLUL; also known as glutamine synthetase, GS) (38, 39) in peri-portal and peri-central areas, respectively (39, 40) (Figure 6A). The liver-type glutaminase (glutaminase-2, GLS2) is activated by ammonia in portal blood and catabolizes glutamine into glutamate, amplifying ammonia concentrations in peri-portal hepatocytes which then detoxify ammonia through CPS1 and the urea cycle (40) (Figure 6A). Excess ammonia that

is not used for urea synthesis by peri-portal hepatocytes is taken up by a small population of peri-central hepatocytes (so-called “perivenous scavenger cells”) that specifically express GS (encoded by the gene, *GLUL*) and convert ammonia into glutamine, thereby preventing ammonia egress into the systemic circulation. Compared to freshly isolated primary hepatocytes, hepatocytes that are reprogrammed to become fetal-like and spheroid-forming by proinflammatory cytokines (TNFα, IL1β, or TNFα + IL1β) express significantly lower levels of *Cps1* and *Glul* (Figure 6B). Accordingly, conditioned medium from the hepatocyte spheroids contains significantly lower levels of urea and glutamine, and considerably higher levels of ammonia than conditioned medium from primary hepatocytes (Figure 6C), indicating that the ammonia detoxifying pathway is impaired in the fetal-like hepatocytes. To confirm the reproducibility of these results, we re-analyzed publicly available scRNA-seq data from hepatocyte spheroids (35) and confirmed that “PRIMARY” hepatocytes strongly express *Cps1* and *Glul*, while both the number of cells expressing these genes, and the level of gene expression per cell, are reduced when hepatocytes are cultured under TNFα-enriched conditions that promote adult-to-fetal reprogramming and spheroid growth (“EXP”) (Figure 6D). Further, switching cultures to TNFα-depleted conditions that promote hepatocyte re-differentiation (“IND”), restores both expression of the ammonia detoxification pathway and *Esrp2* (Figure 6D), demonstrating that these responses are strictly correlated (Supplemental Figure 6D). Importantly, results from the *ex vivo* system recapitulate the changes in ammonia detoxifying genes that occur in human SAH, as evidenced by qRT-PCR data showing that *CPS1* and *GLUL* mRNAs are significantly downregulated in livers of SAH patients compared to healthy controls (Figure 6E). To investigate whether ESRP2 directly regulates ammonia-detoxifying mechanisms, we compared these parameters in uninjured livers of wild-type (WT) and *Esrp2*-KO mice. Hepatic expression of both *Cps1* and *Glul* mRNAs is inhibited significantly by knocking out *Esrp2.* However, this is insufficient to erode ammonia detoxification because serum levels of ammonia and urea are not

significantly different in *Esrp2*-KO mice versus WT mice (Figure 6F,G). On the other hand, *Esrp2*-KO mice have significantly reduced serum levels of albumin (ALB), a soluble protein made by the liver, indicating that some adult hepatocyte functions are suppressed in *Esrp2*-depleted hepatocytes, even in the absence of liver injury (Figure 6G).

Patients with SAH also often exhibit impaired blood clotting. Further, the severity of the coagulopathy is a predictor of short term mortality in SAH (41, 42). Consistent with this, RNA-seq data from explanted human SAH livers demonstrate profound suppression of hepatic genes encoding coagulation factors, and the patients with these failing livers have extremely high levels of prothrombin time (PT) and international normalized ratio (INR) (Figure 1B, Supplemental Figure 2, Supplemental Table 1). To determine if clotting factor synthesis might also be defective in mouse hepatocytes that have undergone fetal reprogramming we examined scRNA-seq data of hepatocyte spheroids and found that fetal-like hepatocytes are also unable to express coagulation factors (*F2, F5, F9, F10, F11, F12, F13b*) and factors that regulate coagulation factors (*Proc, Pros1*) (Supplemental Figure 7), mimicking the loss of clotting factor gene expression in human SAH livers. These results provide further evidence that the fetal reprogramming of adult hepatocytes that occurs in SAH has profound functional significance, contributing to the evolution of life-threatening liver failure in patients with SAH.

Adult-to-fetal reprogramming is a common response to tissue injury

To determine whether ESRP2 suppression and adult-to-fetal reprogramming are specific responses to alcohol-induced liver injury or also occur in other types of liver disease, we treated mice with either vehicle (control) or carbon tetrachloride (CCl_4) for 6 weeks to evoke chronic peri-venous (zone 3) liver injury and induce progressive liver fibrosis. A progressive decrease in ESRP2 expression occurs in zone 3 hepatocytes that survive CCl_4-mediated hepatotoxicity. This is accompanied by progressive accumulation of fetal RNA splicing variants of the HKs and EMT-related genes (*Arhgef10l*, *Slk*, *Kras*), and activation of YAP/TAZ (as evidenced by increased

expression of YAP/TAZ target genes, *Areg*, *Birc5)* (Supplemental Figure 8A-C). mRNA expression of liver progenitor markers, *Igf2bp3* and *Sox9*, is also significantly greater in livers of CCl_4-treated mice than in livers of vehicle-treated controls. Immunostaining for SOX9 confirms that extensive adult-to-fetal reprogramming occurs in response to CCl_4-injury and demonstrates an accompanying accumulation of Cyclin D1 (CCND1)-positive hepatocytes (Supplemental Figure 8D,E). Repopulation of the liver with these proliferative, relatively immature hepatocytes reduces net expression of several adult hepatocyte genes and is accompanied by decrease in related liver functions. For example, mRNA expression of *Glul* (which helps to detoxify ammonia by converting it to glutamine) is virtually abolished in CCl_4-treated mouse livers (Supplemental Figure 8F) and mRNA levels of *Cps1* (which detoxifies ammonia by converting it to urea) tends to be down-regulated, although this does not achieve statistical significance (Supplemental Figure 8F). Nevertheless, serum levels of glutamine decrease significantly in the CCl_4 model (43) and serum concentrations of urea are significantly lower in CCl_4-treated mice than control mice (Supplemental Figure 8G). Serum levels of total bilirubin are also elevated in CCl_4-treated mice, further supporting the concept that some loss of liver-specific functions occurs when persistent suppression of ESRP2 promotes sustained de-differentiation of hepatocytes in this type of liver injury (Supplemental Figure 8G).

We also examined whether *Esrp2* suppression and adult-to-fetal reprogramming occur in kidney tissues of mice with severe liver injury caused by CCl_4, since inflammatory cytokines that increase in the blood of mice with CCl_4-induced liver injury (44) are known to impair renal function in sepsis (45, 46) and many etiologies of advanced liver disease, including SAH, where renal dysfunction is highly predictive of mortality (47, 48). Interestingly, we found that *Esrp2* tends to be suppressed, the fetal splicing variant of a *Kras* (a direct mRNA target of ESRP2) accumulate, and YAP/TAZ are activated, leading to significantly increased expression of YAP/TAZ target genes (*Areg*, *Ptgs2*, *Birc5*) in kidneys of mice with CCl_4-liver injury compared to control mice with healthy livers (Supplemental Figure 9A,B). Considerably more research is required to delineate the role of

ESRP2 in the pathogenesis of renal dysfunction associated with severe liver injury, but our provocative initial findings suggest a novel mechanism that may contribute to the development of hepatorenal syndrome (HRS) in patients with life-threatening SAH (i.e., cytokine-mediated suppression of renal *Esrp2* and consequent adult-to-fetal reprogramming of mature renal epithelial cells).

Depleting ESRP2 in adult hepatocytes exacerbates fetal reprogramming in alcohol-injured livers

Evidence linking the loss of *Esrp2* to suppression of adult RNA splicing programs that control vital adult liver functions, such as ammonia detoxification and clotting factor synthesis, suggests that *Esrp2* may determine susceptibility to SAH. Therefore, we compared functionally-relevant markers of adult-to-fetal reprogramming in WT and *Esrp2*-KO mice at the end of the Gao binge model of AH, which increases exposure to pro-inflammatory cytokines, including TNFα and IL1β (49). In livers of WT mice with AH, *Esrp2* decreases, as expected. Half of the adult splicing events in the six ESRP2 targets that we examined are suppressed, including one HK mRNA (*Csnk1d*) and two EMT-related genes (*Slk*, *Arhgef10l*), and expression of YAP/TAZ target genes (*Areg*, *Birc5*) increases slightly, but not significantly (Figure 7A-C). On the other hand, livers of *Esrp2*-KO mice are enriched with fetal splicing variants of all six ESRP2 target mRNAs, including both HK mRNAs (*Csnk1d*, *Nf2*) and all four EMT-related genes (*Slk*, *Arhgef10l*, *Flnb*, *Kras*) (Figure 7C). In addition, YAP/TAZ target genes (*Fgf1*, *Itgb2*) are significantly upregulated by the end of the alcohol treatment period (Figure 7A). Thus, in livers of mice with AH, there are dose-dependent relationships between decreased ESRP2, increased fetal RNA splicing variants, and activation of YAP, a factor that has been proven to stimulate adult hepatocytes to dedifferentiate into proliferative fetal-like progenitor cells that co-express hepatocyte and ductal cell markers. Therefore, we examined whether the hepatocytes of *Esrp2*-KO mice are more proliferative and fetal-like than WT hepatocytes after alcohol-induced liver injury. Immunohistochemistry for

CCND1 demonstrates rare CCND1(+) hepatocytes in WT mice before alcohol feeding and shows that proliferative hepatocytes increase in WT livers with AH. As expected (12), *Esrp2*-KO hepatocytes are more proliferative than WT hepatocytes at baseline. Further, livers of *Esrp2*-KO mice become massively repopulated by proliferative hepatocytes after alcohol exposure (Figure 8). Immature hepatocytes expressing the ductal marker, SOX9, are barely detected in either WT or *Esrp2*-KO mice before alcohol feeding, although mature-appearing bile duct cells themselves strongly express SOX9 in both groups (Figure 8). After alcohol exposure, both WT and *Esrp2*-KO mice accumulate SOX9(+) hepatocytes and a SOX9(+) ductular-type reaction emerges in *Esrp2*-KO mice (Figure 8). Hence, the aggregate data suggest that ESRP2-depleted hepatocytes are primed to be reprogrammed into proliferative fetal-like cells and confirm that loss of ESRP2 exacerbates fetal reprogramming induced by alcohol, supporting the tenet that ESRP2 mediates susceptibility to liver dysfunction related to AH. To verify that these responses result from direct effects of ESRP2 suppression in hepatocytes, we silenced *Esrp2* in AML12 cells and confirmed that directly inhibiting ESRP2 in hepatocytes increases fetal splicing variants, up-regulates expression of multiple YAP/TAZ target genes (*Areg*, *Cyr61*, *Ctgf*, *Fgf1*, *Itgb2*), and induces various markers of proliferative progenitor cells (*Ccnd1*, *Ck7*, *Snail*, *Vim*, *EpCAM*) (Supplemental Figure 10A-D).

Depleting ESRP2 exacerbates alcohol-induced steatohepatitis in mice

Depleting ESRP2 clearly enhances susceptibility to injury-related de-differentiation of hepatocytes and this compromises liver function. However, whether repopulating the liver with immature cells influences other outcomes of liver injury remains uncertain. Therefore, we treated *Esrp2*-KO mice and WT mice with alcohol according to the Gao binge model of AH and compared liver injury, steatosis, inflammation, and fibrosis. Alcohol treatment increases serum levels of alanine transaminase (ALT) comparably in WT and *Esrp2*-KO mice, suggesting that the severity of alcohol-induced liver injury is not determined by *Esrp2* (Figure 9A). Hepatic steatosis also

increases significantly after alcohol treatment in both groups of mice as assessed by hepatic triglyceride quantification and oil-red-O (ORO) staining (Figures 9B,C). However, liver TG content and ORO staining are greater in *Esrp2*-KO mice than WT mice, and we found that *Esrp2*-depleted livers express higher mRNA levels of peroxisome proliferator-activated receptor gamma (*Ppar*γ) (Figure 9D), a transcription factor that induces lipid accumulation in the liver (50), suggesting that depleting *Esrp2*-KO enhances susceptibility to hepatic steatosis. As mentioned earlier, *Esrp2*-KO mice also develop a more robust ductular reaction than WT mice after chronic alcohol consumption (Figures 8 and 9C). The intensities of the ductular reaction, liver inflammation, and liver fibrogenesis typically correlate with each other (51) because immature liver cells themselves produce chemokines, as well as pro-fibrogenic and pro-inflammatory factors, to promote wound healing responses in damaged livers (5, 7). Consistent with these data, expression of genes encoding inflammatory cytokines (*Tnf*α, *Il1*β) and markers of macrophages (*Cd68*) and neutrophils (*Ly6G*) are upregulated in the livers of alcohol-fed *Esrp2*-KO mice, while none of these genes are significantly induced in the livers of WT mice after alcohol feeding (Figure 9E). mRNA levels of genes encoding fibrosis markers (*Col1*α*1*, *Snail*) are also significantly upregulated in alcohol-injured livers of *Esrp2*-KO mice (Figure 9F), although the Gao binge model of AH causes relatively mild injury and no detectable liver fibrosis (52). Together, the findings in mice confirm that alcohol-induced liver injury promotes suppression of ESRP2 and support the concept that the intensity of the resultant wound-healing response parallels the level of ESRP2 suppression, adult-to-fetal reprogramming, and liver repopulation by immature liver cells. Taken together, our results reveal a novel mechanism that may explain why acute liver failure sometimes develops in individuals who drink alcohol excessively and identify TNFα, IL1β, and ESRP2 as critical regulators of that process (Figure 10).

Discussion

One month mortality rates in patients hospitalized with severe acute alcoholic hepatitis (SAH) are higher than those reported for many other potentially fatal diseases, including myocardial infarction, stroke, and most cancers (53, 54). Death results from progressive and global loss of normal liver functions in SAH, as evidenced by the fact that early replacement of the damaged liver restores both acute and long-term survival (55). Unfortunately, liver transplantation is not an option for most SAH patients, and thus, effective medical therapies are desperately needed. However, developing a successful treatment for SAH has proven challenging due to uncertainties regarding the pathogenesis of SAH-related acute liver failure. In this study, we demonstrate that lethal liver failure in SAH is caused by massive accumulation of immature hepatocytes and identify mechanisms that critically control that process, thereby revealing novel diagnostic and therapeutic targets in this deadly disease. Based on these findings, we also propose a new model for the pathogenesis of acute liver failure in SAH whereby TNFα and IL1β, inflammatory cytokines that are increased by excessive alcohol ingestion, massively suppress ESRP2, an adult RNA splicing factor that maintains the non-proliferative, mature phenotype of adult hepatocytes (Figure 10). The loss of ESRP2 function permits re-emergence of a fetal RNA splicing program that enables hepatocytes that survive alcohol-injury to shed adult hepatocyte functions in order to become more regenerative and heal alcohol-related liver damage. However, vital liver functions are dangerously eroded, and overall survival is threatened when this regenerative response is so exuberant that the liver becomes excessively populated by functionally-immature hepatocytes.

Multiple lines of evidence support this proposed model. Most importantly, mRNA and protein levels of ESRP2, an RNA binding protein that is selectively expressed in mature hepatocytes, are drastically reduced in explanted livers of patients who required urgent liver transplantation to survive SAH. ESRP2 expression and activity are also decreased in several mouse models of AH and the level of ESRP2 suppression correlates with the intensity of alcohol exposure and severity of liver inflammation, supporting the tenet that alcohol-inducible pro-inflammatory cytokines down-

regulate ESRP2. Studies in cultured adult hepatocytes confirm these findings as TNFα and IL1β directly inhibit *Esrp2*. Further research is needed to evaluate the effects of other cytokines on hepatocyte reprogramming.

Critically pertinent to the pathogenesis of liver failure, reducing ESRP2 in hepatocytes has profound functional consequences. In human SAH livers which are massively populated by ESRP2-depleted hepatocytes, key adult RNA splicing programs are replaced by fetal programs, the hepatic transcriptome demonstrates global loss of mature liver functions, and signaling pathways that promote EMT and growth of immature cells are induced. Similar responses accompany ESRP2 suppression in the mouse AH models. These adult-to-fetal phenotypic "switches" are direct consequences of ESRP2 inhibition because they are recapitulated in cultured adult hepatocytes by knocking down *Esrp2* with siRNA or treating the cells with TNFα/IL1β to suppress ESRP2 expression. Further, the de-differentiation process is reversed by re-introducing *Esrp2*. It is particularly noteworthy that suppressing ESRP2 in cultured hepatocytes directly inhibits their expression of clotting factors and blocks ammonia detoxification given that coagulopathy and hyperammonemia are potentially lethal consequences of liver failure and predict acute mortality in SAH (36, 56).

Previous and ongoing research suggest that suppression of ESRP2 is a conserved response to liver injury. For example, we reported that after partial hepatectomy, subpopulations of regenerating mouse hepatocytes transiently suppress their expression of ESRP2 and mature hepatocyte markers (e.g., C/EBPα) but acquire markers of fetal-like cells (e.g., IGF2BP3, YAP and SOX9) (16). That paper also describes striking accumulation of ESRP2-negative hepatocytes in explanted livers from patients with drug-induced acute liver failure. In addition, others recently reported RNA-seq data which demonstrate that *Esrp2* transcripts are significantly decreased in patients with nonalcoholic steatohepatitis compared to control subjects without known liver disease (57). Here we show that hepatic expression of both *Esrp2* mRNA and ESRP2 protein is

inhibited in a mouse model of toxin-induced liver injury. In aggregate, these data indicate that accumulation of ESRP2-negative hepatocytes and the extent of hepatocyte de-differentiation generally parallel the intensity and duration of liver injury and predict the severity of liver dysfunction.

ESRP2 expression is not strictly restricted to liver epithelia (58, 59). Thus, our new evidence that ESRP2 expression is directly suppressed by TNFα and IL1β may also have implications for the pathogenesis of extra-hepatic organ failure in patients with liver injury given that circulating levels of inflammatory cytokines, as well as lipopolysaccharide and other cytokine-inducing factors, increase in many liver diseases (47, 60). Alcohol consumption *per se* can also increase systemic exposure to gut-derived inflammatory signals by disrupting the intestinal epithelial barrier (61). Similarly, sepsis provokes systemic inflammation even in the absence of liver injury (62). Further, our results show that tissues that become repopulated by ESRP2-deficient, fetal-like cells develop a microenvironment that promotes local inflammation and fibrogenesis. Our findings in kidneys from mice with chronic CCl_4-induced liver injury support the tenet that cytokine-mediated adult-to-fetal epithelial reprogramming may generally be involved in inflammation-related organ dysfunction and justify further research to assess the potential role of ESRP2 in the pathogenesis of multiple organ failure. The results will be particularly pertinent for SAH patients because SAH is known to increase the risk for developing the hepatorenal syndrome (HRS), progressive kidney failure, and high short-term mortality (63-65). Moreover, increased levels of circulating cytokines, including TNFα and IL1β, have already been implicated as biomarkers for susceptibility to HRS in SAH patients (65-67) and therapies that inhibit evolution of HRS have been reported to improve survival in SAH (47, 68).

Evidence that ESRP2 suppression promotes SAH mortality fundamentally shifts current paradigms for liver failure pathogenesis because the loss of ESRP2 enhances, rather than inhibits, the viability and regenerative capabilities of adult hepatocytes. Thus, contrary to the conventional

dogma, livers do not fail in patients with fatal SAH because inflammatory cytokines are cytotoxic. Instead, these livers fail because inflammatory cytokines (e.g., TNFα and IL1β) disrupt molecular signaling programs that normally constrain de-differentiation of adult hepatocytes, causing functional parenchyma to be replaced by the fetal-like cells that are lacking liver-specific functions. In this regard, failing SAH livers functionally resemble livers where normal parenchyma is replaced by malignant cells, except that the fetal-like hepatocytes in SAH can re-acquire their mature phenotype after the factors that caused them to de-differentiate dissipate. This helps to explain how it is possible to survive SAH, and why conditions that exacerbate cytokine exposure (e.g., infections and recurrent alcohol abuse) increase SAH mortality (34, 60). Paradoxically, despite all the evidence indicating a significant role for ESRP2 suppression in cytokine-mediated liver failure, ESRP2 is completely dispensable for survival in the absence of liver injury because *Esrp2*-KO mice do not develop liver failure spontaneously. Further*, Esrp2* is suppressed transiently when the liver regenerates after partial hepatectomy (PH) (16) and over-expressing ESRP2 in hepatocytes blocks regeneration and causes progressive liver damage after injury (12). The latter observations may explain why abrogating TNFα signaling also proved to be deadly in SAH (69, 70).

In summary, we have identified a previously unexpected role for an RNA binding protein, ESRP2, in the pathogenesis of SAH-related liver failure, demonstrated how ESRP2-dependent RNA splicing programs critically influence liver functioning after alcohol-injury, and showed for the first time that this process is directly regulated by TNFα and IL1β, inflammatory cytokines that mediate SAH pathogenesis. These findings reveal tractable targets that might be modulated to optimize recovery from SAH while emphasizing the need for further research to map the signaling networks that regulate hepatocyte plasticity in adulthood.

Methods

Human subjects

This study evaluated 6 healthy donor liver tissues and 6 liver tissues from SAH patients who were referred for liver transplantation at Johns Hopkins University Hospital, Baltimore, MD.

RNA-sequencing analysis

RNA-sequencing analysis was performed using high-quality RNA samples from 5 patients with SAH and 5 healthy controls as described (deposited in NCBI GEO database with accession number GSE143318). Genes were considered as having significant differential expression following imposed cutoff clearance (False Discovery rate (FDR) < 0.05, |Log2 (Fold change)| > 0.6). KEGG pathway analysis and annotation of gene tissue expression were performed using DAVID (version 6.8) (71, 72), and mapped using “Enrichment Maps” plugin in Cytoscape (version 3.7.1) (73).

Animal studies

Male WT C57BL/6J (Jackson Laboratory, Bar Harbor, ME) and *Esrp2*-KO mice (University of Illinois Urbana-Champaign, Urbana, IL) generated as previously (13) were fed with short-term chronic (10 days) and one binge ethanol (the NIAAA or Gao binge model) as described in Bertola et. Al. (52). Briefly, both WT (n=12) and *Esrp2*-KO mice (n=10) were initially fed the control Lieber-DeCarli diet *ad libitum* for 5 days to acclimatize them to the liquid diet. Subsequently, ethanol-fed groups were allowed free access for 10 days to the ethanol diet containing 5% (v/v) ethanol, and control groups were pair-fed with the isocaloric control diet. At day 11, ethanol-fed and pair-fed mice received a single dose of ethanol (5 g/kg body weight) or isocaloric maltose dextrin, respectively, via gavage in the early morning and were sacrificed 9 hours later. The HFD±EtOH model was also generated as described previously (5, 74). Briefly, male WT mice (Jackson

Laboratory, Bar Harbor, ME) were fed high-fat liquid diets (HFD) with or without EtOH via continuous intragastric infusion for 4 weeks. The liver tissues were collected for subsequent analyses.

Dr. Hidekazu Tsukamoto (University of Southern California, Los Angeles, CA) and Dr. Ivan Rusyn (Texas A&M University, College Station, TX) provided frozen mouse liver tissues from Tsukamoto-French model or DDC ± EtOH model, respectively. Briefly, the Tsukamoto-French model was generated by permitting mice to consume a high fat/high cholesterol Western diet *ad libitum* for 2 weeks, followed by intra-gastric infusion of EtOH liquid diet (27g/kg/day) for 8 weeks with weekly EtOH binges (4-5 g/kg) started from the second week of intra-gastric feeding. Control mice were administered isocaloric diet without EtOH and gavaged with dextrin maltose (75). The DDC±EtOH model was generated by feeding male wild-type (WT) C57BL/6J mice with 0.05% of DDC diet or base diet for 8 weeks. Animals then underwent surgical intra-gastric intubation (76). After surgery, mice were housed in individual metabolic cages and allowed 2 weeks to recover with *ad libitum* access to food and water. Afterwards, to sub-groups of DDC diet-fed mice, either control high-fat diet or ethanol (EtOH) was delivered continuously through the intragastric cannula up to at 24 g/kg/day by gradually increasing dose for 4 weeks.

To generate a type of severe nonalcoholic liver injury, C57BL/6 mice were treated with 0.6 ml/kg carbon tetrachloride (CCl_4) (n=7 mice) or corn oil (n=4 mice) as vehicle by intraperitoneal injection, twice a week for 6 weeks. Liver and kidney tissues and blood samples were collected for subsequent analyses.

qRT-PCR and splice isoform analysis

Total RNAs were isolated from whole liver tissues or cell lysates using AllPrep DNA/RNA/miRNA Universal Kit (Qiagen, Hilden, Germany) or TRIzol reagent (Invitrogen, Carlsbad, CA). The concentration and purity of RNA were determined using NanoDrop 2000 (ThermoFisher Scientific). Template complementary DNAs were synthesized from total RNA using the High-

Capacity cDNA Reverse Transcription Kit (Applied Biosystems, Foster City, CA) according to the manufacturer's protocols. Platinum II Hot-Start Green PCR Master Mix (Invitrogen) was used for polymerase chain reaction (PCR)-based alternative splicing assays and Power SYBR Green Master Mix (Applied Biosystems) was used for real-time quantitative PCR (qPCR) on the manufacturer's specifications (StepOnePlus™ Real-Time PCR System, Applied Biosystems). PSI values for the variably spliced region were calculated with CS Analyzer 4 software (ATTO Corporation, Tokyo, Japan) as ((exon inclusion band intensity)/(exon inclusion band intensity + exon exclusion band intensity) ×100). The qRT-PCR results were normalized to the housekeeping gene 40S ribosomal proteins S9 (RPS9) mRNA based on the threshold cycle (C_t) and relative fold-change was determined using the $2^{-\Delta\Delta Ct}$ method. The sequences of primers used in this study are listed in Supplemental Table 2.

Cultures of mouse hepatocyte cell line

AML12 cells (ATCC, Old Town Manassas, VA) were cultured in Dulbecco's modified Eagle's medium/F12 Medium (Gibco, ThermoFisher Scientific) supplemented with 10% fetal bovine serum (Gibco), 1× pre-mixed insulin-transferrin-selenium (Gibco), 40 ng/ml dexamethasone and 1× gentamycin (Gibco) at 37 ^{o}C in a humidified atmosphere containing 5% CO_2. Cells were serum starved for 16 hours before treatment. Post serum starvation, cells were released in reduced serum (1% FBS) for up to 48 hours. For knockdown experiments, ON-TARGETplus SMARTpool siRNA for mouse *Esrp2* (GE Healthcare Dharmacon, Inc., Lafayette, CO) or ON-TARGETplus Non-targeting Control Pool (Dharmacon) were purchased. AML12 cells were transfected with gene-specific siRNA oligos (20 nM) using Lipofectamine RNAiMAX (Invitrogen) and 48 hours after transfection, cells were lysed for RNA and protein assays. For TNFα and IL1β treatment, AML12 cells were cultured with or without recombinant murine TNFα (100 ng/ml, Peprotech, Rochky Hill, NJ), IL1β (100 ng/ml, Peprotech) or the combination of TNFα and IL1β (50 ng/ml each, total 100

ng/ml) and harvested after 24 hours for subsequent analyses. Cell proliferation assay was performed using commercial Cell Counting Kit-8 (CCK8) (Dojindo Molecular Technologies, Inc., Kumamoto, Japan).

Co-cultures between AML12 cells and RAW264.7 cells (mouse macrophage cell line from ATCC) were conducted using Transwell inserts (Corning Inc., Corning, NY) in which culture medium was diffusible, but cells were not permeable. RAW264.7 cells were added into transwell inserts above monolayers of AML12 cells, and they were co-cultured for 24 hours. After then, AML12 cells were lysed for subsequent analysis and the levels of TNFα in conditioned medium were evaluated with a commercial ELISA kit for mouse TNFα (Invitrogen) according to the manufacturer's instructions.

Spheroid culture of primary mouse hepatocytes

Primary mouse hepatocytes were isolated from healthy livers of WT male mice using a two-step collagenase perfusion technique as described previously (16). Briefly, mice were anaesthetized with isoflurane to immobilize in the recumbent position on a treatment table, and the inferior vena cava was cannulated under aseptic conditions and the portal vein was cut. Livers were perfused *in situ* with EGTA at 37 °C and then collagenase type IV (Roche, Basel, Switzerland) in phosphate buffered saline (PBS, Gibco). After the liver was digested, it was dissected out, cut into small pieces, and passed through a 100-μm strainer. Hepatocytes were separated from non-parenchymal cells by gravity sedimentation. The purity of the isolated hepatocytes was evaluated with an assessment of the relative percentage of hepatocytic appearing cells using standard microscopy, and this is typically >96% regardless of the timing of hepatocyte isolation.

For the 3D culture of primary mouse hepatocytes, we followed the protocols previously reported by Peng et. Al.(35). Primary mouse hepatocytes were embedded in growth factor reduced matrigel (BD, Franklin Lakes, NJ) at approximately 20,000 cells per well in 24-well plate. To expand hepatocyte spheroids, 3 μM CHIR99021 (Peprotech), 25 ng/ml EGF (Peprotech) and 50

ng/ml HGF (Peprotech) were added to the basal medium described as following: William's E medium containing 1% (v/v) Glutamax (Gibco), 1% (v/v) Non-Essential Amino Acids (Gibco), 1% (v/v) penicillin/streptomycin (Gibco), 0.2% (v/v) normocin (Invitrogen), 2% (v/v) B27 (Gibco), 1% (v/v) N2 supplement (Gibco), 10 mM nicotinamide (Sigma-Aldrich), 1.25 mM N-acetylcysteine (Sigma-Aldrich), 10 μM Y27632 (Peprotech) and 1 μM A83-01 (Tocris Bioscience, Bristol, United Kingdom). To examine the effect of TNFα and IL1β on hepatocyte expansion, 100 ng/ml TNFα or IL1β (Peprotech) was also included to the expansion medium. In some experiments, adenoviruses expressing mouse ESRP2 or GFP as a control were transduced into hepatocyte spheroids under TNFα-mediated expansion condition. Medium was replaced every 2-3 days.

For qRT-PCR and splice isoform analysis from the hepatocyte spheroids, spheroids were harvested from matrigel using dispase (Stem Cell Technologies, Vancouver, Canada) and total RNA was extracted using the RNeasy mini kit (Qiagen) according to the manufacturer's instructions. Following steps were same as described above.

For whole mount immunofluorescence staining, hepatocyte spheroids were processed and stained as described by others (77). Briefly, culture medium was aspirated, hepatocyte spheroids were fixed with 10% formalin and permeabilized after growth for 14 days. Fixed spheroids were blocked in normal goat serum according to the species in which secondary antibody was raised, followed by overnight incubation with primary antibodies (rabbit anti-YAP or rabbit anti-TAZ that were used for immunohistochemistry) at 4 °C. At day 2, spheroids were washed three times and incubated with secondary antibody conjugated with red fluorescein (goat anti-rabbit IgG Alexa Fluor 647, Invitrogen) for 2 hours. After several washes, one droplet of VECTASHIELD Antifade Mounting Medium with DAPI (Vector Laboratories Inc., Burlingame, CA) was added and images were visualized using fluorescence microscope.

Single cell RNA sequencing analysis

Single cell RNA sequencing was performed using the 10x Genomics Chromium System. The Cell Ranger Software (Version 2.1.1) was used to perform sample de-multiplexing, barcode processing and 3' UMI counting. For primary hepatocytes ("PRIMARY"), we removed cells with less than 200 expressed genes, less than 1800 UMIs as well as cells with fraction of mitochondrial UMIs (>20%). Approximately 4,500 cells were sequenced. For expansion culture ("EXP") and induction culture ("IND"), datasets derived from one male and one female were obtained from GEO database with accession numbers GSE120067, and was previously described here (35). Data was reprocessed using Cell Ranger software with mm10 as the reference genome. Single cell data was integrated and analyzed using the workflow from the Seurat R Package (78). The top 10 principal components by PCA analysis were selected for downstream clustering analysis. UMAP plots were used to visualize the clusters.

Statistics

Data are expressed as mean ± s.e.m., unless otherwise specified. Statistical significance between two groups was analyzed by two-tailed Student's *t* test, whereas comparisons of multiple groups were evaluated by one-way or two-way analysis of variance (ANOVA) as specified followed by a *post-hoc* Tukey's test. Correlations were assessed by Pearson's correlation coefficient (*r*). *p*-values < 0.05 were considered statistically significant. Drawing graphs and statistical analyses were performed using GraphPad Prism 8 (GraphPad Software, Inc. La Jolla, CA, USA).

Study approval

The human research was approved by Human Ethics Committee of Johns Hopkins University Hospital (IRB 00107893), and written informed consent was obtained from all participants. Human samples were used in accordance with the National Institutes of Health and institutional guidelines

for human subject research. Animal studies were conducted under the approved Duke University (A262-18-11) and University of Illinois, Urbana-Champaign Institutional Animal Care and Use Committee (IACUC) protocols as per the National Research Council ‘Guide for the Care and Use of Laboratory Animals’.

Author contributions

JH designed the research studies, conducted experiments, acquired data, analyzed data, provided reagents, wrote and revised the manuscript; ZS and ARA provided human liver samples and RNA-seq data; SB, KD, UC, TC conducted experiments and acquired data; HT and IR provided mouse liver samples; AK provided reagents and *Esrp2*-KO mice, conducted some of the alcohol feeding studies and provided funding to support some of the alcohol feeding studies; AMD designed the research studies, analyzed data, wrote and revised the manuscript, secured funding for the research.

Acknowledgments

This work was supported by NIH grants DK106633, AA010154, DK077794 to AMD and HL126845 to AK and R24 AA025017 to ZS, the Florence McAlister Professorship of Medicine (AMD), a Planning Grant Award from Cancer Center at Illinois (AK), a postdoc fellowship from the Duke Regeneration Next Initiative (JH), the NIH Tissue microenvironment training program T32-EB019944 (SB), and the Animal Core of the NIAAA Alcohol Research Center at USC (HT).

References

1. Louvet A, and Mathurin P. Alcoholic liver disease: mechanisms of injury and targeted treatment. *Nat Rev Gastroenterol Hepatol.* 2015;12(4):231-242.
2. Yu C-H, Xu C-F, Ye H, Li L, and Li Y-M. Early mortality of alcoholic hepatitis: a review of data from placebo-controlled clinical trials. *World J Gastroenterol.* 2010;16(19):2435-2439.
3. Orntoft NW, Sandahl TD, Jepsen P, and Vilstrup H. Short-term and long-term causes of death in patients with alcoholic hepatitis in Denmark. *Clin Gastroenterol Hepatol.* 2014;12(10):1739-1744. e1731.
4. Altamirano J, Fagundes C, Dominguez M, García E, Michelena J, Cárdenas A, et al. Acute kidney injury is an early predictor of mortality for patients with alcoholic hepatitis. *Clin Gastroenterol Hepatol.* 2012;10(1):65-71. e63.
5. Jung Y, Brown KD, Witek RP, Omenetti A, Yang L, Vandongen M, et al. Accumulation of hedgehog-responsive progenitors parallels alcoholic liver disease severity in mice and humans. *Gastroenterology.* 2008;134(5):1532-1543.
6. Sancho-Bru P, Altamirano J, Rodrigo-Torres D, Coll M, Millán C, José Lozano J, et al. Liver progenitor cell markers correlate with liver damage and predict short-term mortality in patients with alcoholic hepatitis. *Hepatology.* 2012;55(6):1931-1941.
7. Aguilar-Bravo B, Rodrigo-Torres D, Ariño S, Coll M, Pose E, Blaya D, et al. Ductular reaction cells display an inflammatory profile and recruit neutrophils in alcoholic hepatitis. *Hepatology.* 2019;69(5):2180-2195.
8. Achanta S, Verma A, Srivastava A, Nilakantan H, Hoek JB, and Vadigepalli R. Single cell gene expression analysis identifies chronic alcohol-mediated shift in hepatocyte molecular states after partial hepatectomy. *Gene Expr.* 2018;19(2):97-119.
9. Yimlamai D, Christodoulou C, Galli GG, Yanger K, Pepe-Mooney B, Gurung B, et al. Hippo pathway activity influences liver cell fate. *Cell.* 2014;157(6):1324-1338.

10. Yu F-X, Zhao B, and Guan K-L. Hippo pathway in organ size control, tissue homeostasis, and cancer. *Cell.* 2015;163(4):811-828.

11. Shiojiri N, Takeshita K, Yamasaki H, and Iwata T. Suppression of C/EBP α expression in biliary cell differentiation from hepatoblasts during mouse liver development. *J Hepatol.* 2004;41(5):790-798.

12. Bangru S, Arif W, Seimetz J, Bhate A, Chen J, Rashan EH, et al. Alternative splicing rewires Hippo signaling pathway in hepatocytes to promote liver regeneration. *Nat Struct Mol Biol.* 2018;25(10):928-939.

13. Bhate A, Parker DJ, Bebee TW, Ahn J, Arif W, Rashan EH, et al. ESRP2 controls an adult splicing programme in hepatocytes to support postnatal liver maturation. *Nat Commun.* 2015;6:8768.

14. Warzecha CC, Sato TK, Nabet B, Hogenesch JB, and Carstens RP. ESRP1 and ESRP2 are epithelial cell-type-specific regulators of FGFR2 splicing. *Mol Cell.* 2009;33(5):591-601.

15. Horiguchi K, Sakamoto K, Koinuma D, Semba K, Inoue A, Inoue S, et al. TGF-β drives epithelial-mesenchymal transition through δEF1-mediated downregulation of ESRP. *Oncogene.* 2012;31(26):3190-3201.

16. Hyun J, Oh S-H, Premont RT, Guy CD, Berg CL, and Diehl AM. Dysregulated activation of fetal liver programme in acute liver failure. *Gut.* 2019:gutjnl-2018-317603.

17. Wands J, Carter E, Bucher N, and Isselbacher K. Inhibition of hepatic regeneration in rats by acute and chronic ethanol intoxication. *Gastroenterology.* 1979;77(3):528-531.

18. Duguay L, Coutu D, Hetu C, and Joly J. Inhibition of liver regeneration by chronic alcohol administration. *Gut.* 1982;23(1):8-13.

19. Yin M, Wheeler MD, Kono H, Bradford BU, Gallucci RM, Luster MI, et al. Essential role of tumor necrosis factor α in alcohol-induced liver injury in mice. *Gastroenterology.* 1999;117(4):942-952.

20. Karaca G, Xie G, Moylan C, Swiderska-Syn M, Guy CD, Krüger L, et al. Role of Fn14 in acute alcoholic steatohepatitis in mice. *Am J Physiol Gastrointest Liver Physiol.* 2014;308(4):G325-G334.

21. Kawaguchi Y. Sox9 and programming of liver and pancreatic progenitors. *J Clin Invest.* 2013;123(5):1881-1886.

22. Nakagawa H, Hikiba Y, Hirata Y, Font-Burgada J, Sakamoto K, Hayakawa Y, et al. Loss of liver E-cadherin induces sclerosing cholangitis and promotes carcinogenesis. *Proc Natl Acad Sci U S A.* 2014;111(3):1090-1095.

23. Zong Y, Panikkar A, Xu J, Antoniou A, Raynaud P, Lemaigre F, et al. Notch signaling controls liver development by regulating biliary differentiation. *Development.* 2009;136(10):1727-1739.

24. Yang N, Morrison CD, Liu P, Miecznikowski J, Bshara W, Han S, et al. TAZ induces growth factor-independent proliferation through activation of EGFR ligand amphiregulin. *Cell Cycle.* 2012;11(15):2922-2930.

25. Zhang H, Pasolli HA, and Fuchs E. Yes-associated protein (YAP) transcriptional coactivator functions in balancing growth and differentiation in skin. *Proc Natl Acad Sci U S A.* 2011;108(6):2270-2275.

26. Zhao B, Ye X, Yu J, Li L, Li W, Li S, et al. TEAD mediates YAP-dependent gene induction and growth control. *Genes Dev.* 2008;22(14):1962-1971.

27. Zhang H, Liu C-Y, Zha Z-Y, Zhao B, Yao J, Zhao S, et al. TEAD transcription factors mediate the function of TAZ in cell growth and epithelial-mesenchymal transition. *J Biol Chem.* 2009;284(20):13355-13362.

28. Li W, Cao Y, Xu J, Wang Y, Li W, Wang Q, et al. YAP transcriptionally regulates COX-2 expression and GCCSysm-4 (G-4), a dual YAP/COX-2 inhibitor, overcomes drug resistance in colorectal cancer. *J Exp Clin Cancer Res.* 2017;36(1):144.

29. Warzecha CC, Shen S, Xing Y, and Carstens RP. The epithelial splicing factors ESRP1 and ESRP2 positively and negatively regulate diverse types of alternative splicing events. *RNA Biol.* 2009;6(5):546-562.

30. Tranchevent L-C, Aubé F, Dulaurier L, Benoit-Pilven C, Rey A, Poret A, et al. Identification of protein features encoded by alternative exons using Exon Ontology. *Genome Res.* 2017;27(6):1087-1097.

31. Shapiro IM, Cheng AW, Flytzanis NC, Balsamo M, Condeelis JS, Oktay MH, et al. An EMT–driven alternative splicing program occurs in human breast cancer and modulates cellular phenotype. *PLoS Genet.* 2011;7(8):e1002218.

32. Khanova E, Wu R, Wang W, Yan R, Chen Y, French SW, et al. Pyroptosis by caspase11/4-gasdermin-D pathway in alcoholic hepatitis in mice and patients. *Hepatology.* 2018;67(5):1737-1753.

33. Rosenbluh J, Nijhawan D, Cox AG, Li X, Neal JT, Schafer EJ, et al. β-Catenin-driven cancers require a YAP1 transcriptional complex for survival and tumorigenesis. *Cell.* 2012;151(7):1457-1473.

34. Gao B, Ahmad MF, Nagy LE, and Tsukamoto H. Inflammatory pathways in alcoholic steatohepatitis. *J Hepatol.* 2019;70(2):249-259.

35. Peng WC, Logan CY, Fish M, Anbarchian T, Aguisanda F, Álvarez-Varela A, et al. Inflammatory Cytokine TNFα Promotes the Long-Term Expansion of Primary Hepatocytes in 3D Culture. *Cell.* 2018;175(6):1607-1619. e1615.

36. Ravi S, Bade KS, Hasanin M, and Singal AK. Ammonia level at admission predicts in-hospital mortality for patients with alcoholic hepatitis. *Gastroenterol Rep (Oxf).* 2016;5(3):232-236.

37. Aldridge DR, Tranah EJ, and Shawcross DL. Pathogenesis of hepatic encephalopathy: role of ammonia and systemic inflammation. *J Clin Exp Hepatol.* 2015;5:S7-S20.

38. Qvartskhava N, Lang PA, Görg B, Pozdeev VI, Ortiz MP, Lang KS, et al. Hyperammonemia in gene-targeted mice lacking functional hepatic glutamine synthetase. *Proc Natl Acad Sci U S A.* 2015;112(17):5521-5526.

39. Hakvoort T, He Y, Kulik W, Vermeulen JL, Duijst S, Ruijter JM, et al. Pivotal role of glutamine synthetase in ammonia detoxification. *Hepatology.* 2017;65(1):281-293.

40. Massafra V, Milona A, Vos HR, Ramos RJ, Gerrits J, Willemsen EC, et al. Farnesoid X receptor activation promotes hepatic amino acid catabolism and ammonium clearance in mice. *Gastroenterology.* 2017;152(6):1462-1476. e1410.

41. Northup PG, and Caldwell SH. Coagulation in liver disease: a guide for the clinician. *Clin Gastroenterol Hepatol.* 2013;11(9):1064-1074.

42. Kim W, and Kim DJ. Severe alcoholic hepatitis-current concepts, diagnosis and treatment options. *World J Hepatol.* 2014;6(10):688-695.

43. Du K, Chitneni SK, Suzuki A, Wang Y, Henao R, Hyun J, et al. Increased Glutaminolysis Marks Active Scarring in Nonalcoholic Steatohepatitis Progression. *Cell Mol Gastroenterol Hepatol.* 2020.

44. Liu Y, Wen PH, Zhang XX, Dai Y, and He Q. Breviscapine ameliorates CCl4‐induced liver injury in mice through inhibiting inflammatory apoptotic response and ROS generation. *Int J Mol Med.* 2018;42(2):755-768.

45. Murugan R, Karajala-Subramanyam V, Lee M, Yende S, Kong L, Carter M, et al. Acute kidney injury in non-severe pneumonia is associated with an increased immune response and lower survival. *Kidney Int.* 2010;77(6):527-535.

46. Cunningham PN, Dyanov HM, Park P, Wang J, Newell KA, and Quigg RJ. Acute renal failure in endotoxemia is caused by TNF acting directly on TNF receptor-1 in kidney. *J Immunol.* 2002;168(11):5817-5823.

47. Arora R, Kathuria S, and Jalandhara N. Acute renal dysfunction in patients with alcoholic hepatitis. *World J Hepatol.* 2011;3(5):121-124.

48. Altamirano J, Fagundes C, Dominguez M, García E, Michelena J, Cárdenas A, et al. Acute kidney injury is an early predictor of mortality for patients with alcoholic hepatitis. *Clin Gastroenterol Hepatol.* 2012;10(1):65-71. e63.

49. Bertola A, Park O, and Gao B. Chronic plus binge ethanol feeding synergistically induces neutrophil infiltration and liver injury in mice: a critical role for E-selectin. *Hepatology.* 2013;58(5):1814-1823.

50. Zhang W, Sun Q, Zhong W, Sun X, and Zhou Z. Hepatic peroxisome proliferator-activated receptor gamma signaling contributes to alcohol-induced hepatic steatosis and inflammation in mice. *Alcohol Clin Exp Res.* 2016;40(5):988-999.

51. Sato K, Marzioni M, Meng F, Francis H, Glaser S, and Alpini G. Ductular reaction in liver diseases: pathological mechanisms and translational significances. *Hepatology.* 2019;69(1):420-430.

52. Bertola A, Mathews S, Ki SH, Wang H, and Gao B. Mouse model of chronic and binge ethanol feeding (the NIAAA model). *Nat Protoc.* 2013;8(3):627-637.

53. Hughes E, Hopkins LJ, and Parker R. Survival from alcoholic hepatitis has not improved over time. *PLoS One.* 2018;13(2):e0192393.

54. Nguyen TA, DeShazo JP, Thacker LR, Puri P, and Sanyal AJ. The worsening profile of alcoholic hepatitis in the United States. *Alcohol Clin Exp Res.* 2016;40(6):1295-1303.

55. Mathurin P, Moreno C, Samuel D, Dumortier J, Salleron J, Durand F, et al. Early liver transplantation for severe alcoholic hepatitis. *N Engl J Med.* 2011;365(19):1790-1800.

56. Liangpunsakul S. Clinical characteristics and mortality of hospitalized alcoholic hepatitis patients in the United States. *J Clin Gastroenterol.* 2011;45(8):714-719.

57. Hoang SA, Oseini A, Feaver RE, Cole BK, Asgharpour A, Vincent R, et al. Gene Expression Predicts Histological Severity and Reveals Distinct Molecular Profiles of Nonalcoholic Fatty Liver Disease. *Sci Rep.* 2019;9(1):1-14.

58. Mizutani A, Koinuma D, Seimiya H, and Miyazono K. The Arkadia-ESRP2 axis suppresses tumor progression: analyses in clear-cell renal cell carcinoma. *Oncogene.* 2016;35(27):3514-3523.

59. Bebee TW, Park JW, Sheridan KI, Warzecha CC, Cieply BW, Rohacek AM, et al. The splicing regulators Esrp1 and Esrp2 direct an epithelial splicing program essential for mammalian development. *Elife.* 2015;4:e08954.

60. Neuman M, Maor Y, Nanau R, Melzer E, Mell H, Opris M, et al. Alcoholic liver disease: role of cytokines. *Biomolecules.* 2015;5(3):2023-2034.

61. Bishehsari F, Magno E, Swanson G, Desai V, Voigt RM, Forsyth CB, et al. Alcohol and gut-derived inflammation. *Alcohol Res.* 2017;38(2):163-171.

62. Fry DE. Sepsis, systemic inflammatory response, and multiple organ dysfunction: the mystery continues. *Am Surg.* 2012;78(1):1-8.

63. O'Beirne J, Patch D, Holt S, Hamilton M, and Burroughs AK. Alcoholic hepatitis—the case for intensive management. *Postgrad Med J.* 2000;76(898):504-507.

64. Ginès A, Escorsell A, Ginès P, Saló J, Jiménez W, Inglada L, et al. Incidence, predictive factors, and prognosis of the hepatorenal syndrome in cirrhosis with ascites. *Gastroenterology.* 1993;105(1):229-236.

65. Dagher L, and Moore K. The hepatorenal syndrome. *Gut.* 2001;49(5):729-737.

66. Sheron N, Bird G, Koskinas J, Portmann B, Ceska M, Lindley I, et al. Circulating and tissue levels of the neutrophil chemotaxin interleukin-8 are elevated in severe acute alcoholic hepatitis, and tissue levels correlate with neutrophil infiltration. *Hepatology.* 1993;18(1):41-46.

67. Sheron N, Bird G, Goka J, Alexander G, and Williams R. Elevated plasma interleukin-6 and increased severity and mortality in alcoholic hepatitis. *Clin Exp Immunol.* 1991;84(3):449-453.

68. De BK, Gangopadhyay S, Dutta D, Baksi SD, Pani A, and Ghosh P. Pentoxifylline versus prednisolone for severe alcoholic hepatitis: a randomized controlled trial. *World J Gastroenterol.* 2009;15(13):1613-1619.

69. Naveau S, Chollet-Martin S, Dharancy S, Mathurin P, Jouet P, Piquet MA, et al. A double-blind randomized controlled trial of infliximab associated with prednisolone in acute alcoholic hepatitis. *Hepatology.* 2004;39(5):1390-1397.

70. Boetticher NC, Peine CJ, Kwo P, Abrams GA, Patel T, Aqel B, et al. A randomized, double-blinded, placebo-controlled multicenter trial of etanercept in the treatment of alcoholic hepatitis. *Gastroenterology.* 2008;135(6):1953-1960.

71. Huang DW, Sherman BT, and Lempicki RA. Systematic and integrative analysis of large gene lists using DAVID bioinformatics resources. *Nat Protoc.* 2008;4(1):44-57.

72. Huang DW, Sherman BT, and Lempicki RA. Bioinformatics enrichment tools: paths toward the comprehensive functional analysis of large gene lists. *Nucleic Acids Res.* 2008;37(1):1-13.

73. Shannon P, Markiel A, Ozier O, Baliga NS, Wang JT, Ramage D, et al. Cytoscape: a software environment for integrated models of biomolecular interaction networks. *Genome Res.* 2003;13(11):2498-2504.

74. Uesugi T, Froh M, Arteel GE, Bradford BU, and Thurman RG. Toll-like receptor 4 is involved in the mechanism of early alcohol-induced liver injury in mice. *Hepatology.* 2001;34(1):101-108.

75. Lazaro R, Wu R, Lee S, Zhu NL, Chen CL, French SW, et al. Osteopontin deficiency does not prevent but promotes alcoholic neutrophilic hepatitis in mice. *Hepatology.* 2015;61(1):129-140.

76. Kono H, Bradford BU, Rusyn I, Fujii H, Matsumoto Y, Yin M, et al. Development of an intragastric enteral model in the mouse: studies of alcohol-induced liver disease using knockout technology. *J Hepatobiliary Pancreat Surg.* 2000;7(4):395-400.

77. Rezanejad H, Lock JH, Sullivan BA, and Bonner-Weir S. Generation of Pancreatic Ductal Organoids and Whole-Mount Immunostaining of Intact Organoids. *Curr Protoc Cell Biol.* 2019;83(1):e82.

78. Butler A, Hoffman P, Smibert P, Papalexi E, and Satija R. Integrating single-cell transcriptomic data across different conditions, technologies, and species. *Nat Biotechnol.* 2018;36(5):411-420.

Figure legends

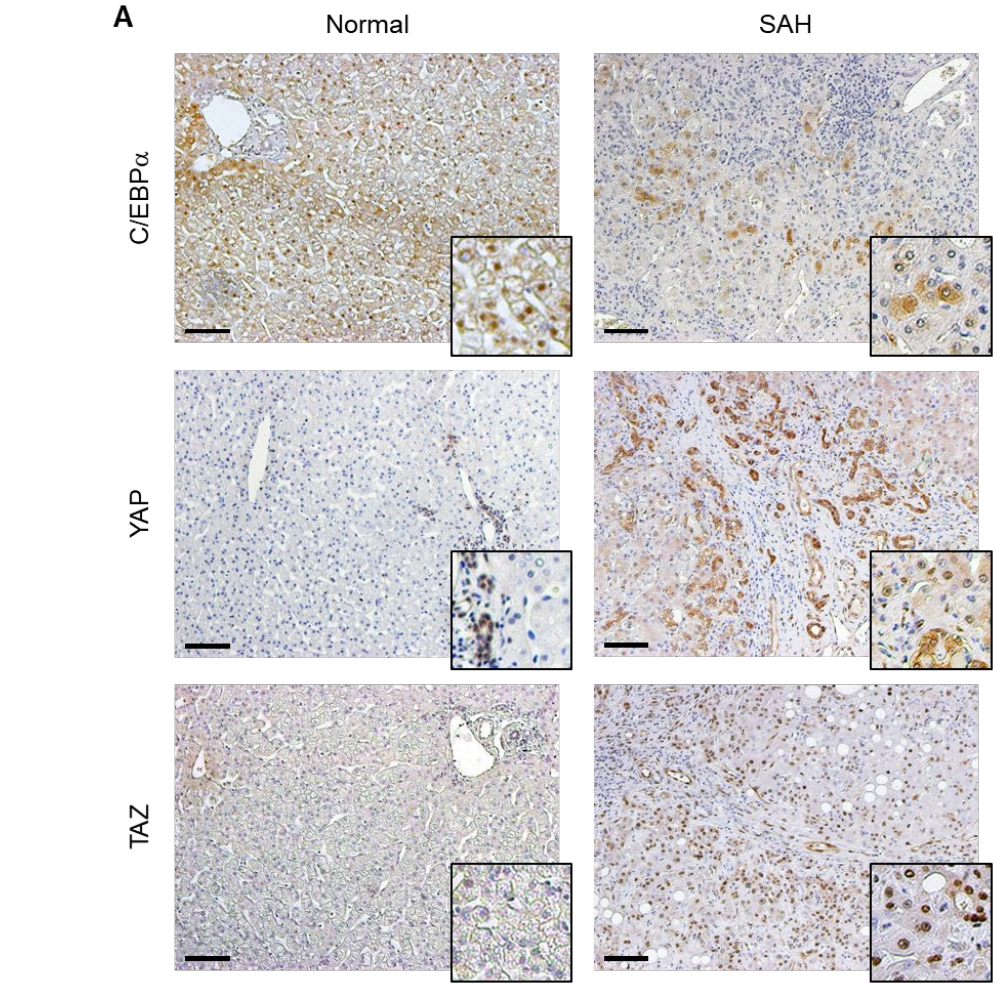

Figure 1. Hepatocytes are fetal-like in patients with severe alcoholic hepatitis. (A) Immunohistochemistry (IHC) for C/EBPα, YAP and TAZ in explanted liver tissues of patients with severe alcoholic hepatitis (SAH) and healthy human liver. Representative images are shown. Scale bar=100μm. Magnification=100×. Each higher magnification image (400×) is shown in right-bottom. **(B)** An enrichment map consisted of KEGG pathways and annotations of tissue expression which are involved by significantly up- (green circle) or down- (blue circle) regulated genes in liver tissues of SAH patients compared to healthy controls (n=5 each) by RNA-seq analysis. The node size is proportionate to the number of genes for each category and thickness of edges is proportionate to the number of shared genes between categories.

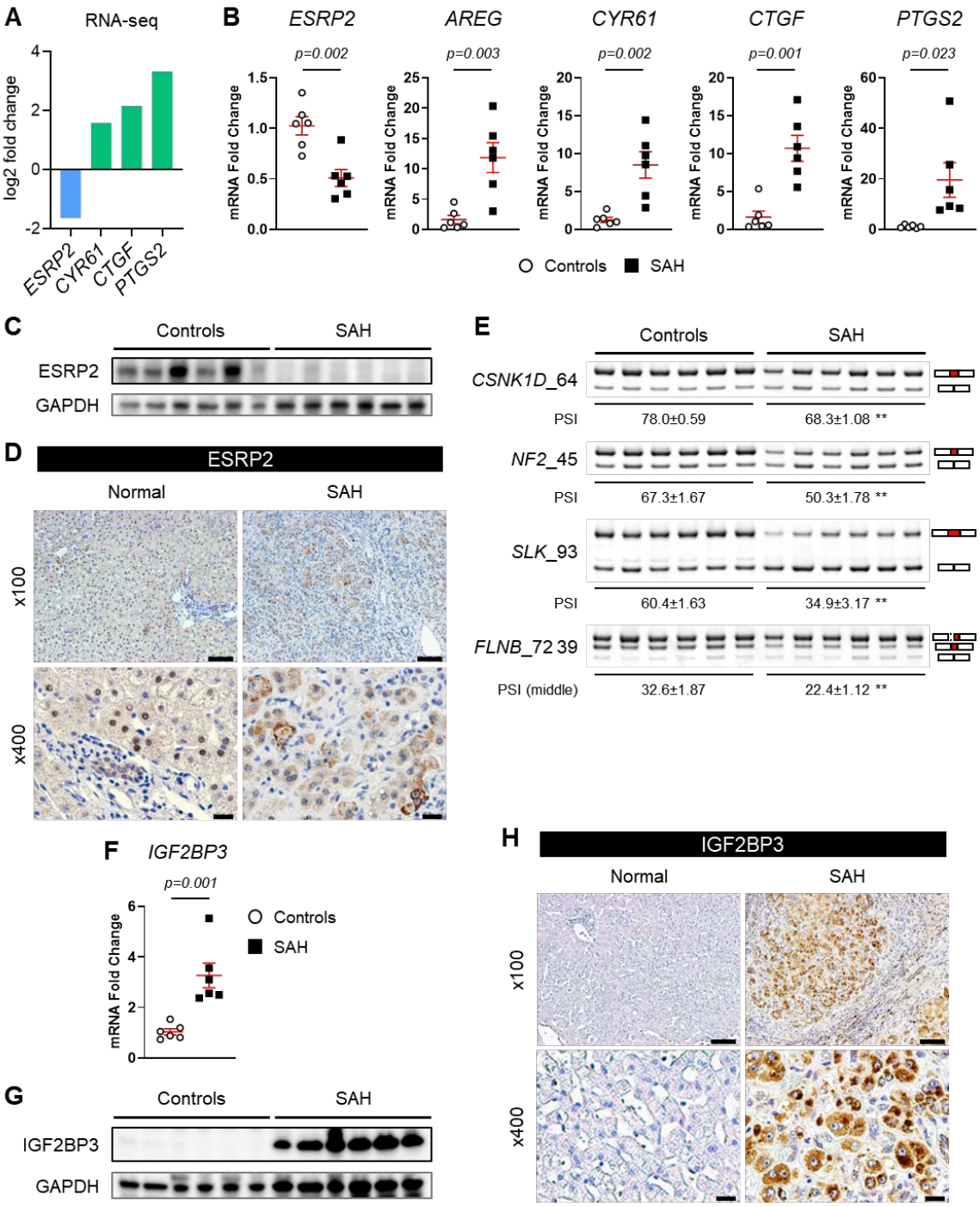

Figure 2. ESRP2 expression and ESRP2-mediated adult RNA splicing program are down-regulated in livers of patients with severe alcoholic hepatitis. (A) Log2 fold changes of *ESRP2* and direct YAP/TAZ target genes (*CYR61*, *CTGF*, *PTGS2*) assessed by RNA-seq in liver explants from SAH patients relative to healthy controls (n=5 each). **(B)** qRT-PCR analysis for

ESRP2 and YAP/TAZ target genes (*AREG*, *CYR61*, *CTGF*, *PTGS2*) in human SAH livers and healthy controls. **(C)** Immunoblots for ESRP2 normalized to GAPDH as a loading control in lysates of liver tissues from SAH patients and healthy controls. **(D)** IHC for ESRP2 in explanted liver tissues of SAH patients and healthy human liver. **(E)** Alternative splicing of ESRP2 target mRNAs including *CSNK1D*, *NF2*, *SLK* and *FLNB* between liver tissues of SAH patients and healthy controls. The upper bands include the exon (red part), while the lower bands skip exon. The exon lengths are shown beside the gene name and the differences in percent spliced in (PSI) values are shown as mean±s.e.m. below each image. **(F-H)** qRT-PCR analysis **(F)**, Immunoblot **(G)**, and IHC **(H)** for IGF2BP3 in the livers of SAH patients and healthy controls. qRT-PCR results are graphed as dot plots (SAH: black square, Healthy controls: white circle) with mean±s.e.m. (red bars) (n=5 individuals/group). Statistical analysis was performed by using two-tailed student *t* test between two groups (n=5 individuals/group, *p* values are specified otherwise, $^{**}p<0.001$). s.e.m., standard error of the mean. Representative images are shown for IHC. Scale bar=100μm for magnification=100×, 20 μm for magnification=400×.

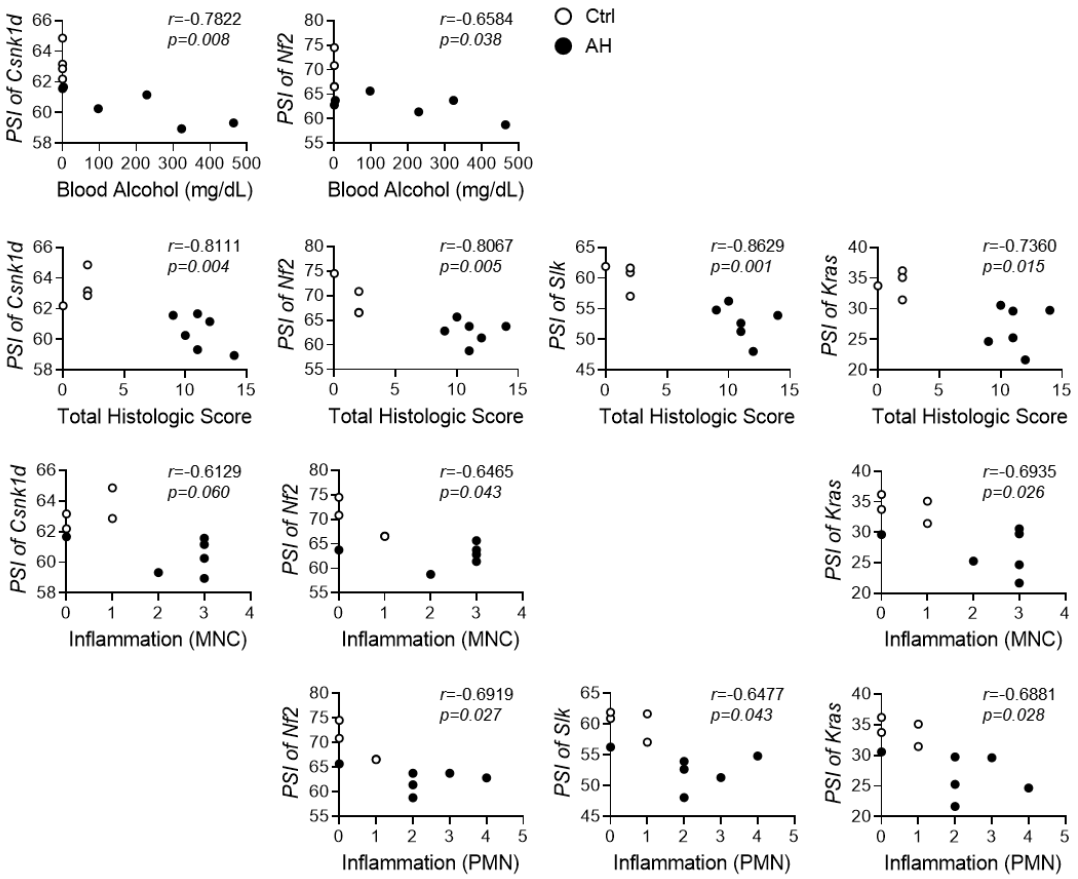

Figure 3. Fetal RNA splicing occurs as increase of alcohol exposure and liver damage in mouse model of alcoholic hepatitis. The Pearson's r correlation analysis between the PSI of *Csnk1d*, *Nf2*, *Slk* or *Kras* in liver tissues and the levels of blood alcohol, total histologic score, or inflammation of control (Ctrl) or alcoholic hepatitis (AH) mice of Tsukamoto-French model (r, correlation coefficient). Results are graphed as dot plots (AH: black square, Ctrl: white circle). MNC, mononuclear cell; PMN, polymorphonuclear neutrophil.

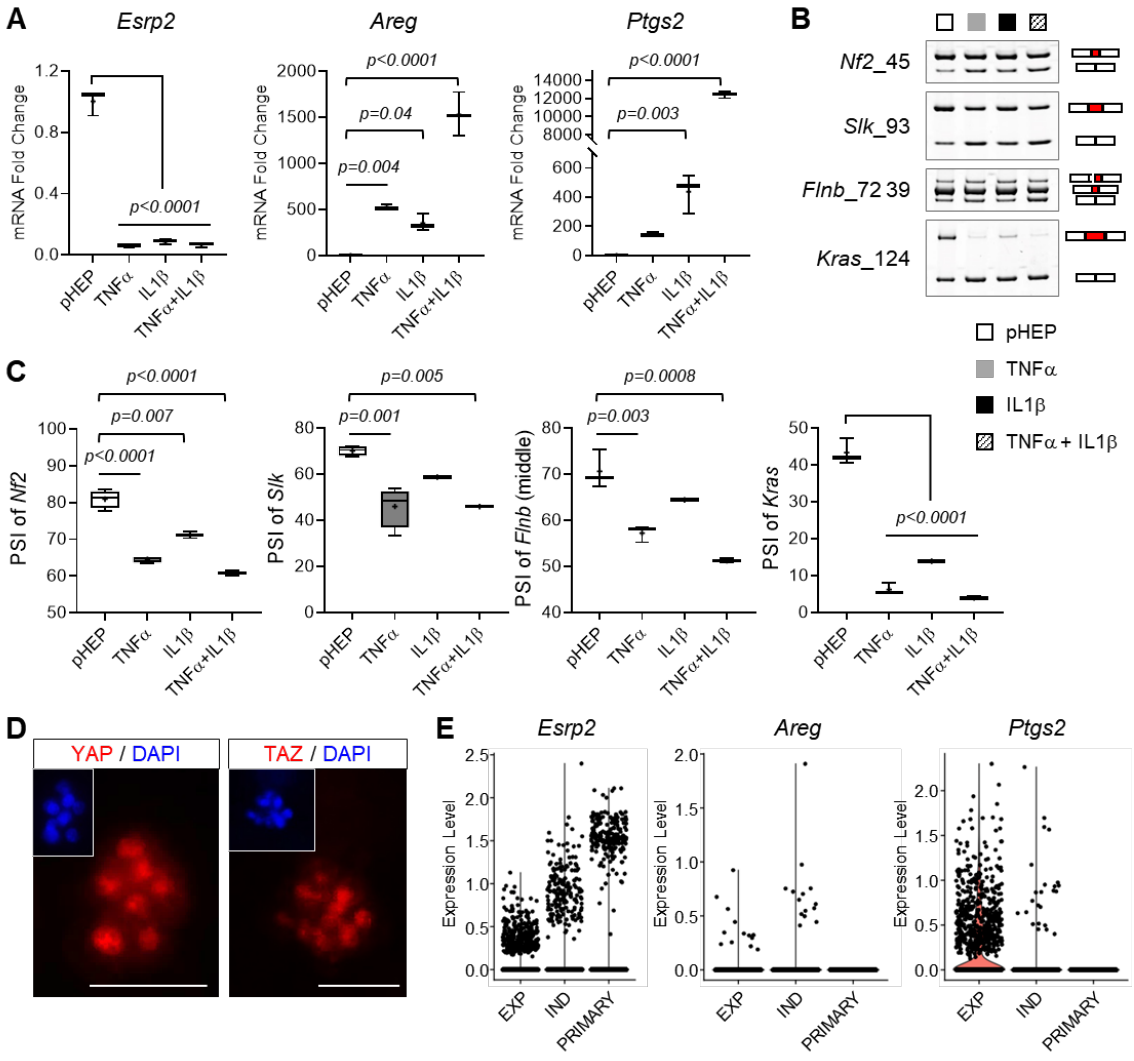

Figure 4. Adult hepatocytes are reprogrammed to fetal-like cells in proinflammatory cytokine-dependent spheroid culture system. (A) qRT-PCR for *Esrp2* and YAP/TAZ target genes (*Areg* and *Ptgs2*) in freshly isolated primary mouse hepatocytes (pHEP) and primary hepatocytes cultured under spheroid-forming system for 18 days continuously treated with TNFα, IL1β, or TNFα + IL1β. Results are graphed as box and whiskers plots (Min to Max), and means are indicated as "+". **(B and C)** Alternative splicing of *Nf2*, *Slk*, *Flnb*, *and Kras* in primary hepatocytes as specified. The representative gel images are shown from at least 3 replicates **(B)**. Results are graphed as box and whiskers plots (Min to Max), and means are indicated as "+" **(C)**. **(D)** Images of hepatocyte spheroids stained for YAP (left, red) and TAZ (right, red) visualized by

whole mount immunofluorescence. Nuclear counterstaining was done by 4',6-diamidino-2-phenylindole (DAPI, blue). Scale bar=50μm. **(E)** scRNA-seq analysis for *Esrp2*, *Areg* and *Ptgs2* in primary hepatocytes ("PRIMARY") and hepatocyte spheroids under TNFα-mediated expansion medium ("EXP") or TNFα-withdrawn induction medium ("IND") as described in a previous publication (35).

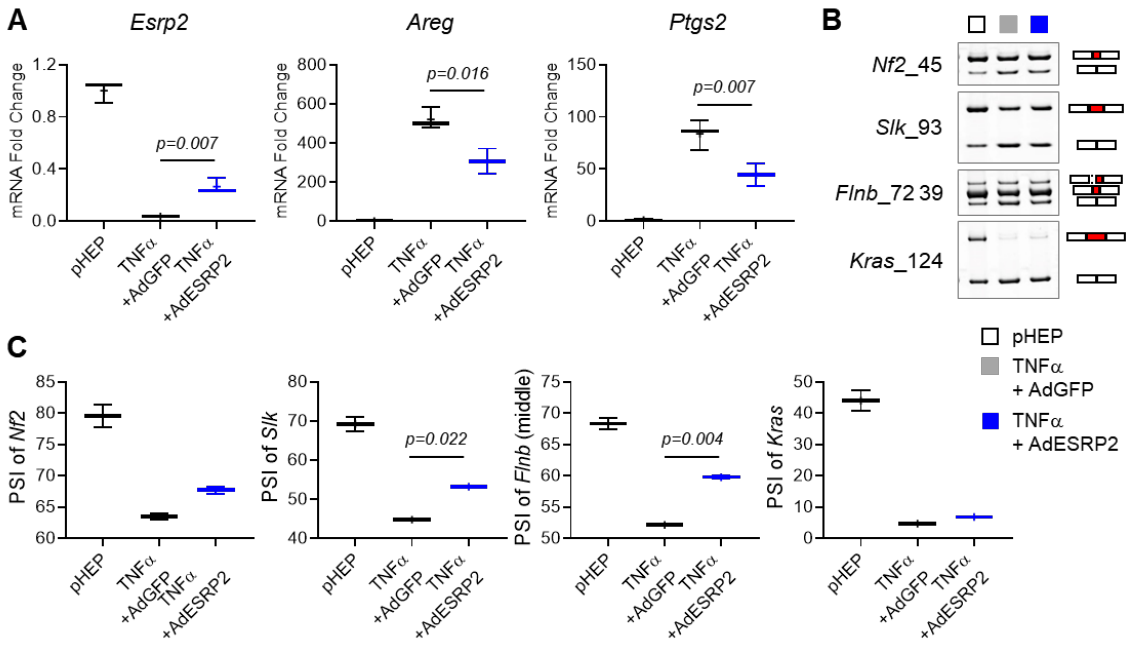

Figure 5. Fetal reprogramming of hepatocytes is mediated by ESRP2-regulated RNA splicing program. (A) qRT-PCR for *Esrp2*, *Areg* and *Ptgs2* in pHEP and TNFα-treated hepatocyte spheroids either transduced with adenoviruses expressing GFP (TNFα + AdGFP) or mouse ESRP2 (TNFα + AdESRP2). Results are graphed as box and whiskers plots (Min to Max), and means are indicated as "+". **(B and C)** Alternative splicing of *Nf2*, *Slk*, *Flnb*, *and Kras* in primary hepatocytes as specified, and "pHEP" samples were shared with Figure 4B **(B)**. Results are graphed as box and whiskers plots (Min to Max), and means are indicated as "+" **(C)**. All statistical analyses were performed by one-way analysis of variation (ANOVA) with Tukey corrections (n=3 biological replicates/group).

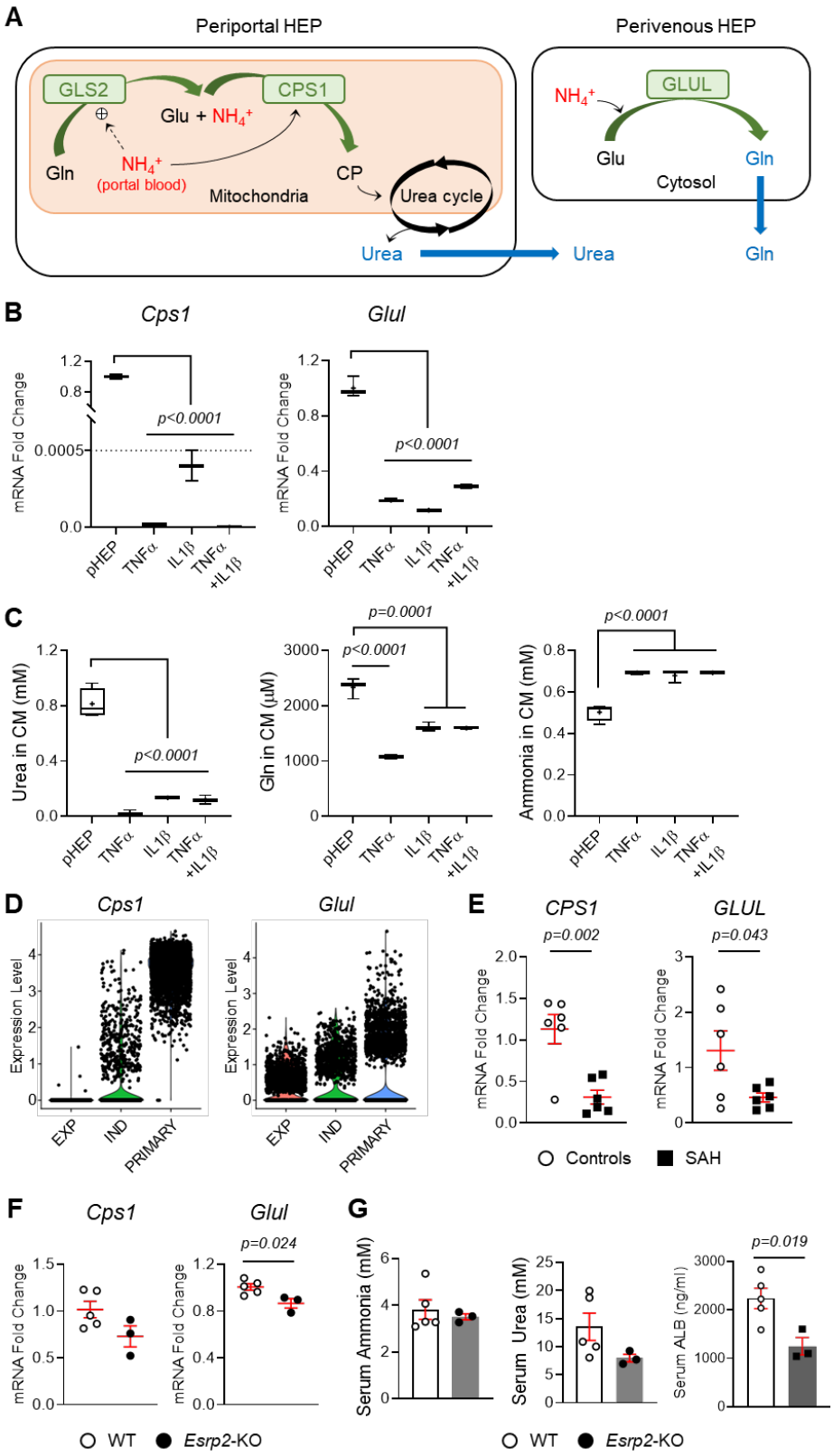
A
Periportal HEP
Perivenous HEP
GLS2
CPS1
Glu + NH4+
Gln
NH4+
(portal blood)
Mitochondria
CP
Urea cycle
Urea
NH4+
GLUL
Glu
Gln
Cytosol
Urea
Gln
B
Cps1
Glul
mRNA Fold Change
p<0.0001
p<0.0001
pHEP
TNFα
IL1β
TNFα +IL1β
C
Urea in CM (mM)
Gln in CM (μM)
Ammonia in CM (mM)
p<0.0001
p=0.0001
p<0.0001
p<0.0001
D
Cps1
Glul
Expression Level
EXP
IND
PRIMARY
E
CPS1
GLUL
p=0.002
p=0.043
mRNA Fold Change
Controls
SAH
F
Cps1
Glul
p=0.024
mRNA Fold Change
WT
Esrp2-KO
G
Serum Ammonia (mM)
Serum Urea (mM)
Serum ALB (ng/ml)
p=0.019
WT
Esrp2-KO

Figure 6. Fetal reprogrammed hepatocytes lose adult liver-specific functions. (A) A schematic of ammonia (NH_4^+) detoxification pathway by hepatocytes in the liver. Glu, glutamate; Gln, glutamine; CP, carbamoyl phosphate; CPS1, carbamoyl phosphate synthetase-1; GLS2, glutaminase-2; GLUL, glutamate-ammonia ligase (also known as glutamine synthetase). **(B)** qRT-PCR analysis for *Cps1* and *Glul* in freshly isolated primary mouse hepatocytes (pHEP) and primary hepatocytes cultured under spheroid-forming system for 18 days continuously treated with TNFα, IL1β, or TNFα + IL1β. **(C)** The levels of urea, glutamine (Gln) and ammonia in conditioned medium of primary hepatocytes as specified. Results are graphed as box and whiskers plots (Min to Max), and means are indicated as "+". Statistical analysis was performed by one-way ANOVA with Tukey corrections (n=3 biological replicates/group). **(D)** scRNA-seq analysis for *Cps1* and *Glul* in primary hepatocytes ("PRIMARY") and hepatocyte spheroids under TNFα-mediated expansion medium ("EXP") or TNFα-withdrawn induction medium ("IND") as described in a previous publication (35). **(E)** qRT-PCR analysis for *CPS1* and *GLUL* in human livers with severe alcoholic hepatitis (SAH) and healthy controls. Results are graphed as dot plots (SAH: black square, Healthy controls: white circle) with mean±s.e.m. (red bars) (n=5 individuals/group). Statistical analysis was performed by using two-tailed student *t* test between two groups. **(F)** qRT-PCR analysis for *Cps1* and *Glul* in mouse livers from wild-type (WT) and *Esrp2* knock out (KO) mice at baseline. Results are graphed as dot plots (*Esrp2*-KO: black circle, WT: white circle) with mean±s.e.m. (red bars) (n=3-5 individuals/group). Statistical analysis was performed by using two-tailed student *t* test between two groups. **(G)** The serum levels of ammonia, urea and albumin (ALB) in healthy WT and *Esrp2*-KO mice. The mean±s.e.m. results are graphed, and the statistical analysis was performed by using two-tailed student *t* test between two groups (n=3-5 mice/group).

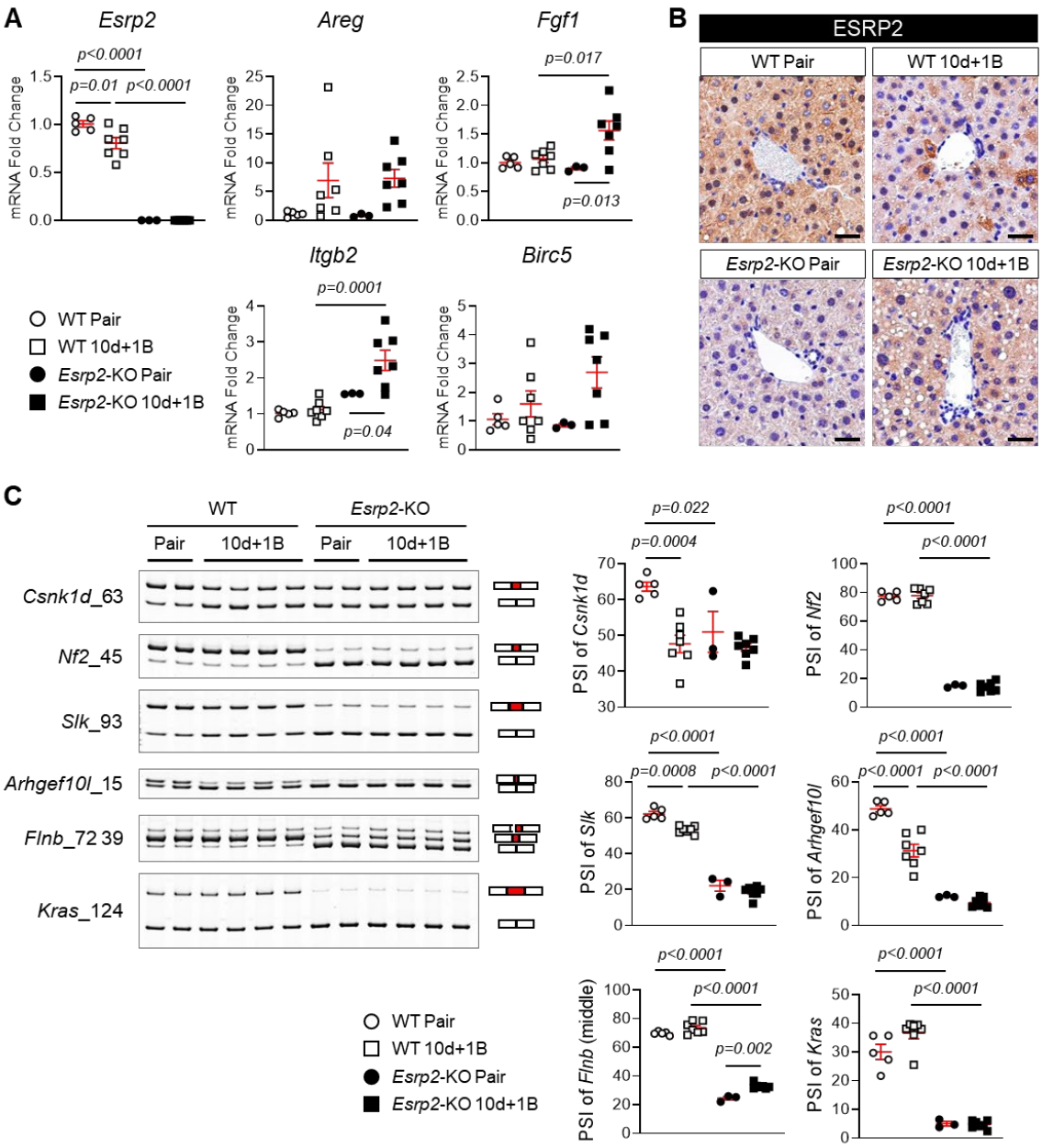

Figure 7. Loss of ESRP2 promotes adult-to-fetal switch in Gao Binge model. (A) qRT-PCR analysis for *Esrp2* and YAP/TAZ target genes (*Areg*, *Fgf1*, *Itgb2* and *Birc5*) in WT and *Esrp2*-KO mice exposed to 10 days feeding and one binge drinking of ethanol (10d + 1B) and pair-fed mice. **(B)** IHC for ESRP2 in liver sections from these mice. Scale bar=100μm. **(C)** Alternative splicing for HK mRNAs and EMT-related genes (*Slk*, *Arhgef10l*, *Flnb* and *Kras*) in WT and *Esrp2*-KO Gao Binge mouse models. All results are graphed as dot plots (WT Pair: white circle, WT 10d+1B:

white square, *Esrp2*-KO Pair: black circle, *Esrp2*-KO 10d+1B: black square) with mean±s.e.m. (red bars) (n=3-7 individuals/group). All statistical analyses were performed by two-way analysis of variation (ANOVA) with Tukey corrections.

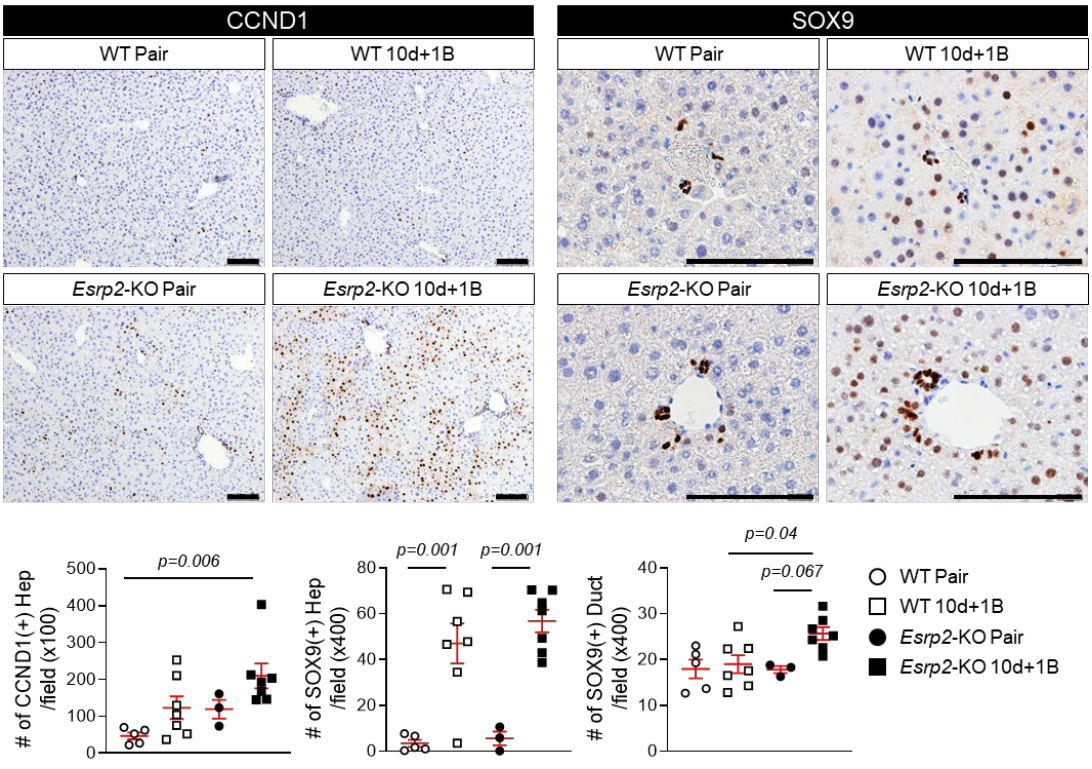

Figure 8. ESRP2-depleted hepatocytes become proliferative ductal-like cells after alcohol exposure. IHC for CCND1 and SOX9 in liver sections of WT and *Esrp2*-KO mice with or without alcohol exposure. The numbers of CCND1-positive hepatocytes (Hep) and SOX9-positive liver cells (hepatocytes, Hep; ductal cells, Duct) were counted in >10 randomly selected 100× or 400× fields per each section, respectively. Scale bar=100μm. Results are graphed as dot plots (WT Pair: white circle, WT 10d+1B: white square, *Esrp2*-KO Pair: black circle, *Esrp2*-KO 10d+1B: black square) with mean±s.e.m. (red bars) (n=3-7 individuals/group). Statistical analyses were performed by two-way analysis of variation (ANOVA) with Tukey corrections.

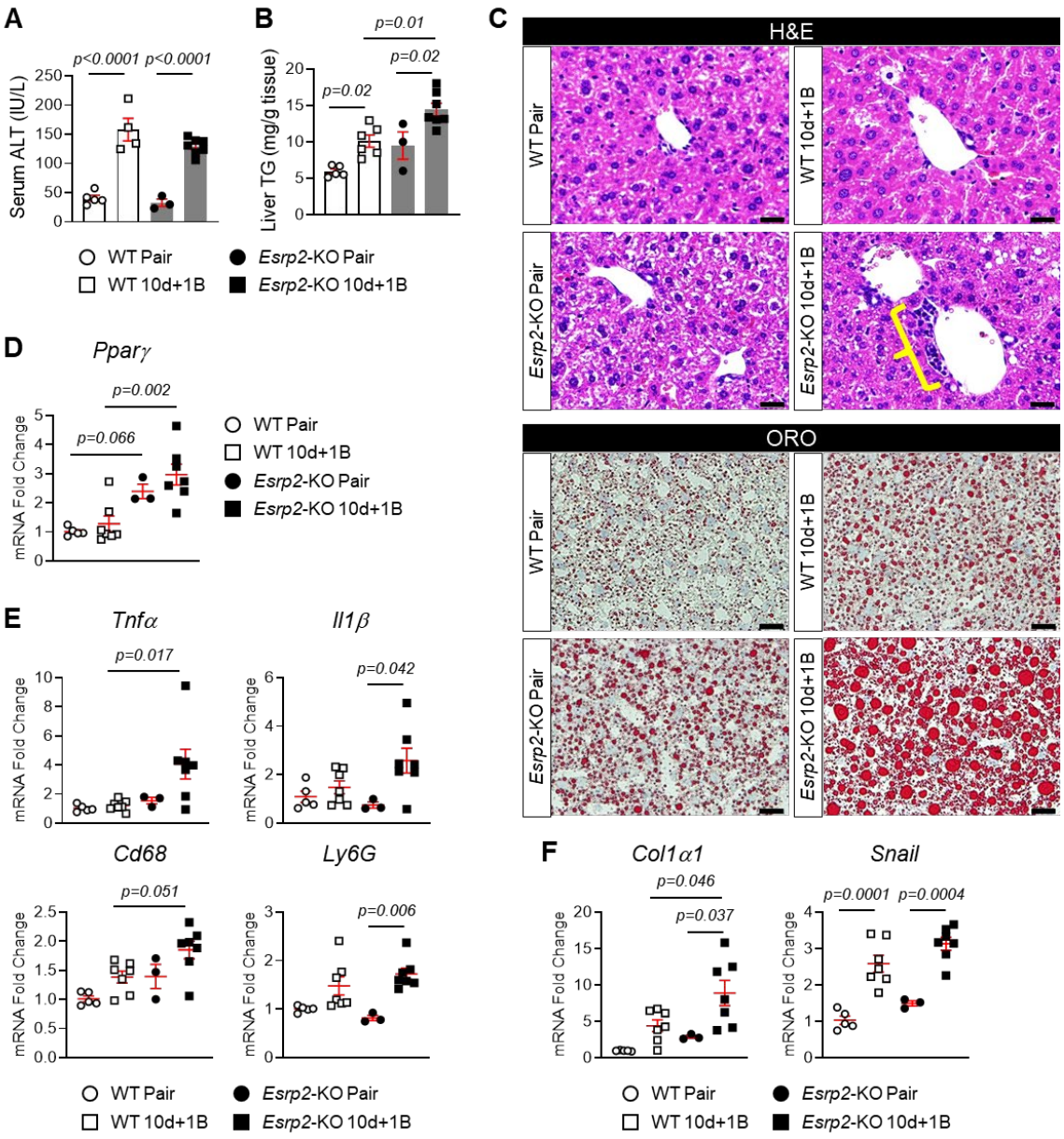

Figure 9. Depleting ESRP2 exacerbates alcohol-induced steatohepatitis in mice. (A) The serum levels of alanine transaminase (ALT) in WT and *Esrp2*-KO mice treated with alcohol as per the Gao binge model. Results are graphed as dot plots (WT Pair: white circle with white bar, WT 10d+1B: white square with white bar, *Esrp2*-KO Pair: black circle with gray bar, *Esrp2*-KO 10d+1B: black square with gray bar) with mean±s.e.m. (red bars) (n=3-7 individuals/group). **(B)** Hepatic triglyceride (TG) content in WT and Esrp2-KO mice with or without alcohol exposure. **(C)** Hematoxylin and eosin (H&E) and oil red O (ORO) staining in liver sections of these mice. Yellow

bracket indicates the ductular reaction. Scale bars=20μm. **(D, E and F)** qRT-PCR analysis for *Ppar*γ **(D)**, inflammatory cytokines (*Tnf*α and *Il1*β) and immune cell markers (*Cd68* and *Ly6G*) **(E)**, and fibrogenic markers (*Col1*α*1* and *Snail*) **(F)** in WT and *Esrp2*-KO mice exposed to alcohol or pair- fed control diet. All results are graphed as dot plots (WT Pair: white circle, WT 10d+1B: white square, *Esrp2*-KO Pair: black circle, *Esrp2*-KO 10d+1B: black square) with mean±s.e.m. (red bars) (n=3-7 individuals/group). All statistical analyses were performed by two-way analysis of variation (ANOVA) with Tukey corrections.

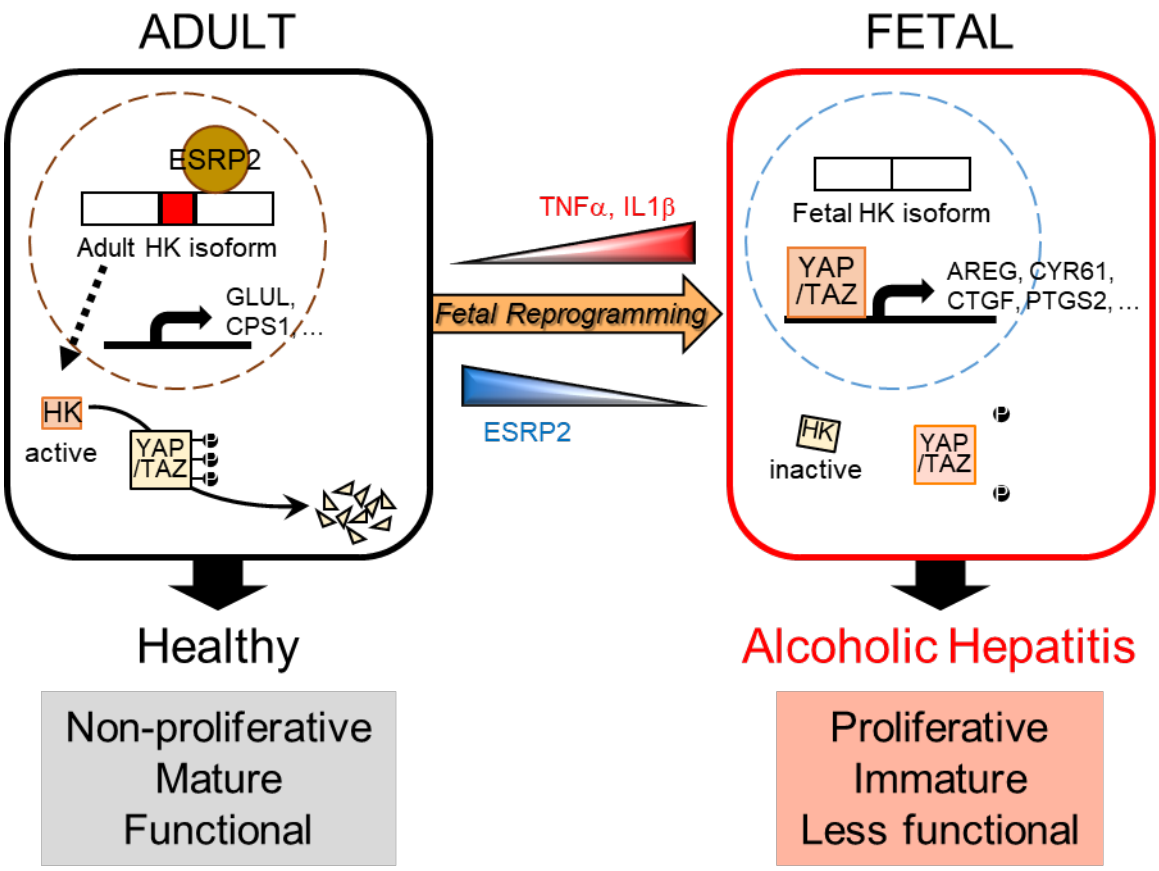

Figure 10. Model for liver failure in severe acute alcoholic hepatitis (SAH). Inflammatory cytokines, such as TNFα and IL1β, suppress ESRP2, an adult RNA splicing factor. Loss of ESRP2 permits fetal RNA splicing variants of hippo kinases (HKs) to accumulate. Because fetal HKs are relatively inactive, phosphorylation and clearance of their targets, YAP/TAZ, are impaired, allowing these fetal transcription factors to accumulate and re-activate fetal gene expression programs. Thus, the surviving adult hepatocytes are reprogrammed to become more fetal-like and regenerative, but less mature. This provokes loss of critical adult hepatocyte functions, including ammonia detoxification and clotting factor biosynthesis, and causes the clinical features of liver failure.